

---

# Intravital microscopy of lung ischemia reperfusion injury in a rat model

Rongrui Na

---



München 2021

Aus der Herzchirurgischen Klinik und Poliklinik  
Klinik der Ludwig-Maximilians-Universität München Großhadern  
Vorstand: Prof. Dr. med. Christian Hagl

*Intravital microscopy of lung ischemia reperfusion  
injury in a rat model*

Dissertation  
zum Erwerb des Doktorgrades der Medizin  
an der Medizinischen Fakultät der  
Ludwig-Maximilians-Universität zu München

vorgelegt von

Rongrui Na

aus

Sichuan

2021

Mit Genehmigung der Medizinischen Fakultät  
der Universität München

Berichterstatter: Prof. Dr. med. René Schramm, PhD

Mitberichterstatter: PD Dr. med. habil. Tobias Heer

Dekan: Prof. Dr. med. dent. Reinhard HICKEL

Tag der mündlichen Prüfung: 14.01.2021

## **CONTENTS**

<b>1.</b>	<b>Abstract</b>	<b>1</b>
<b>2.</b>	<b>Zusammenfassung</b>	<b>2</b>
<b>3.</b>	<b>Introduction</b>	<b>3</b>
<b>3.1.</b>	<b>Lung transplantation</b>	<b>3</b>
<b>3.2.</b>	<b>Pulmonary ischemia-reperfusion injury</b>	<b>4</b>
<b>3.3.</b>	<b>Intravital fluorescence microscopy (IVM)</b>	<b>10</b>
<b>4.</b>	<b>Aim of the study</b>	<b>14</b>
<b>5.</b>	<b>Materials and Methods</b>	<b>15</b>
<b>5.1.</b>	<b>Animals</b>	<b>15</b>
<b>5.2.</b>	<b>Experimental procedures</b>	<b>15</b>
<b>5.2.1.</b>	<b>Anesthesia</b>	<b>15</b>
<b>5.2.2.</b>	<b>Microsurgical procedures</b>	<b>16</b>
<b>5.3.</b>	<b>Intravital fluorescence microscopy</b>	<b>17</b>
<b>5.3.1.</b>	<b>Imaging</b>	<b>17</b>
<b>5.3.2.</b>	<b>Parameters</b>	<b>18</b>
<b>5.4.</b>	<b>Histopathological analyses</b>	<b>20</b>
<b>5.5.</b>	<b>Statistical analysis</b>	<b>22</b>
<b>6.</b>	<b>Results</b>	<b>23</b>
<b>6.1.</b>	<b>Intravital fluorescence microscopic imaging (IVM)</b>	<b>23</b>
<b>6.2.</b>	<b>Histopathologic analyses</b>	<b>36</b>
<b>7.</b>	<b>Discussion</b>	<b>43</b>
<b>8.</b>	<b>References</b>	<b>51</b>

## **Abstract**

This thesis establishes and validates an experimental animal model to analyse leukocyte recruitment and microvascular dysfunction in pulmonary ischemia/reperfusion injury by intravital fluorescence microscopy in the rat.

The pleural surface of the rat left lung has been exposed by atraumatic microsurgical techniques and fluorescence epi-illumination was used to visualize subpleural pulmonary microcirculation under baseline conditions and during reperfusion after 30 min of ischemia.

The results show that this experimental setup bears the required spatial and temporal resolution to study postischemic leukocyte responses within the pulmonary microcirculation. All segments of pulmonary microvascular tree can be differentially analysed, including feeding arterioles, alveolar capillaries and draining postcapillary venules. The data analyses demonstrate that the relatively mild ischemic insult of 30 min provokes a detectable leukocytic response, i.e. significantly increased leukocyte-endothelial cell adhesive interactions in postcapillary subpleural pulmonary venules during reperfusion. Microhemodynamics were not significantly altered during reperfusion. These results translate into the histopathological analyses, confirming mild affection of the pulmonary tissue structures after 90 min of reperfusion. Confirming i) the relatively mild ischemic insult to the lung and ii) virtual absence of trauma by the microsurgical preparations, remote organ damage was basically absent the heart and kidney, but only minimally seen in the liver.

In conclusion, the established experimental setup allows for reproducible analyses pulmonary ischemia/reperfusion injury on the microcirculatory level in the rat lung. The use of this basic approach may serve as a reliable basic model for further studies on pulmonary ischemia/reperfusion injury and experimental allo- and xenogeneic lung transplantation.

## **Zusammenfassung**

Im Rahmen dieser Promotionsarbeit wird ein tierexperimentelles Modell zur Analyse von Leukozytenrekrutierung und mikrovaskulärer Dysfunktion während pulmonalem Ischämie/Reperfusionsschaden mittels intravitaler Fluoreszenzmikroskopie in der Ratte etabliert und evaluiert.

Die pleurale Oberfläche der linken Lunge wird durch atraumatischen mikrochirurgischen Techniken exponiert. Mittels Fluoreszenz-epi-Illumination wird die subpleurale Mikrozirkulation der Lunge unter Basisbedingungen und während Reperfusion nach einer 30 minütigen Ischämie visualisiert.

Die Ergebnisse zeigen, dass der experimentelle Ansatz die notwendige räumliche und zeitliche Auflösung besitzt, um die postischämische Leukozytenantwort in der pulmonalen Mikrozirkulation darzustellen. Alle Segmente der pulmonalen mikrovaskulären Strombahn können differenziert analysiert werden. Dies beinhaltet zuführende Arteriolen, alveoläre Kapillaren und drainierende postkapilläre Venolen. Die Datenanalyse zeigt, dass der relative milde 30-minütige, ischämische Insult eine detektierbare Leukozytenantwort provoziert, d.h. significant erhöhte Leukozyten - Endothelzell Adhäsionen in postkapillären pulmonalen Venolen während Reperfusion. Die Mikrohämodynamik war nicht significant beeinträchtigt während Reperfusion. Diese Ergebnisse übersetzen sich in die histopathologische Analysen, eine milde Affektion der Lungengewebestruktur nach 90 Minuten Reperfusion bestätigen. Sekundäre Organschäden in Herz und Niere wurden nicht detektiert und waren nur milde ausgeprägt in der Leber zu finden, was einerseits die relative Milde der Lungenischämie und andererseits die nahezu atraumatischen mikrochirurgische Präparationen bestätigt.

Zusammenfassend erlaubt der experimentelle Ansatz eine reproduzierbare Analyse des Ischämie/Reperfusionsschadens in der Rattenlunge auf mikrovaskulärer Ebene. Dieser Ansatz kann als zuverlässiges experimentelles Basismodell für weitergehende Untersuchungen des Ischämie/Reperfusionsschadens in der Lunge, sowie allo- und xenogener Lungentransplantation dienen.

### **3. Introduction**

#### **3.1. Lung transplantation**

Lung transplantation has become a valid option in the treatment of end-stage lung diseases, refractory to any other medical and/or surgical therapy [1]. Since the first successful clinical transplantation of a donor lung in 1963, the results after lung transplantation for end-stage lung disease have steadily improved. Most recent data indicate a median survival after lung transplantation of 6.7 years and a 1-year survival of 8.9 years [2]. The improved outcome has been achieved by refinements of surgical techniques, e.g. periprocedural use of extracorporeal circulation [3], and advances in immunosuppressive therapy, e.g. introduction of calcineurin inhibitors [4, 5]. Despite all these advances, survival after lung transplantation is still limited and the overall results are far from perfect.

Transplanted lung allografts are damaged in the postoperative and long-term course by several mechanisms (Figure 1). Such include the ischemia/reperfusion injury mediated by the unspecific innate immunity, as well as acute and chronic rejections through specific adaptive immune responses [5, 6]. In addition, donor-specific antibody-mediated rejection episodes may occur, although there is only limited understanding of when and how this entity of post lung transplant organ injury develops and works [7]. Regarding the continuous deterioration of graft function post-transplant, it is a well-established understanding that ischemia/reperfusion injury occurs within the first days after transplantation, while acute cellular rejection episodes may occur at different time points longer-term. However, the highest incidence of acute cellular rejection episodes is within the first 6 to 12 months after lung transplantation [2]. The detailed mechanisms underlying chronic lung allograft rejection are not completely understood at present, but it manifests clinically in steadily declining lung function test parameters and the pathophysiologic correlate is a fibrotic swelling of the terminal bronchioli, previously designated as the bronchiolitis obliterans syndrome. However, more recent definitions of the chronic lung allograft dysfunction (CLAD) further differentiate between more obstructive or restrictive functional and structural destruction of the transplanted lung allograft [8].

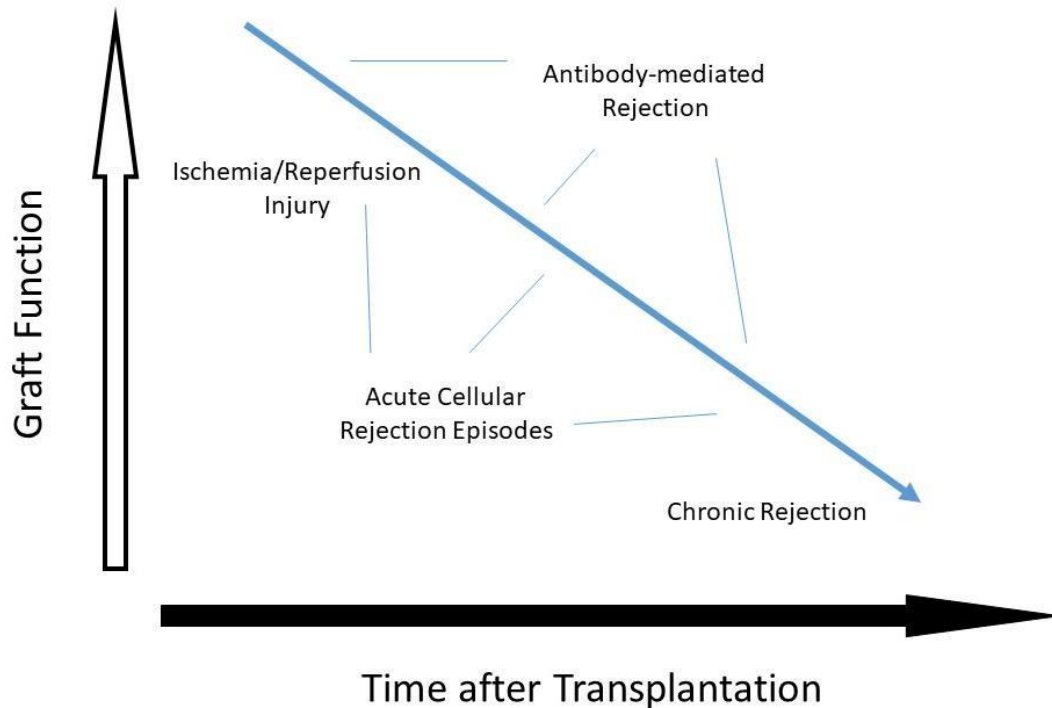


**Figure 1:** Lung injury after transplantation. The function of a transplanted lung allograft is at risk during the early postoperative period due to ischemia/reperfusion injury provided by the innate immune system. The specific and adaptive immune responses trigger the frequency and intensity of acute rejection episodes as well as chronic rejection determining the outcome of lung transplantation long-term.

### 3.2. Pulmonary ischemia-reperfusion injury

#### *Clinical aspects*

The magnitude of the injurious net effect following ischemia during reperfusion primarily depends on and is proportionate to the duration of the anoxic phase following organ retrieval, during transportation and implantation into the recipient [9, 10]. It has been well recognized that tolerance of transplanted organs towards ischemia can be improved by vigorous organ cold preservation, i.e. the organs are perfused in the donor by a chilled preservation solution at the time of retrieval and are transported on ice to the recipient operation. This applies also to lung allografts, in which colloidal, buffered electrolyte solutions are used [11, 12]. However, despite improved procurement techniques and optimal preservation measures, the ischemic time of a lung allograft must not be extended over a maximum of 9 to 12 hours [13, 14], because this would significantly endanger a positive outcome of the transplant procedure.

The transplantation of a lung allograft differs to a certain extent from other solid organ transplantations as the nutritive arterial vasculature is not connected to the recipients circulation. Only pulmonary arteries carrying deoxygenated blood to the lung are anastomosed. Drainage of blood is conducted through the pulmonary veins into the recipients left atrium. Bronchial arteries derived from the systemic blood stream are not anastomosed [15]. It has been suggested that this reasons, why mainly the bradytroph bronchial tissue is at risk during severe ischemia/reperfusion injury of the lung after transplantation, potentially leading to impaired healing of the anastomosed bronchi or even necrotising disruption of this fragile airway connection [15, 16].

Ischemia/reperfusion injury has been considered to manifest clinically as the primary graft dysfunction (PGD) after lung transplantation. It has a reported incidence of between 10%-30% and is a major cause of death in early post-transplantation days [17-19]. According to the 34<sup>th</sup> report of the registry of the International Society for Heart and Lung Transplantation (ISHLT), PGD is one major reason of death within the first 30 days of transplantation [4]. The ISHLT proposed a clinical definition of PGD and that is the presence of hypoxemia and radiographic appearance of diffuse pulmonary opacities in post-transplant chest X-rays without other identifiable causes within the first 72 hours after surgery. Its severity is judged clinically depending on the ratio of arterial oxygen fraction ( $\text{PaO}_2$ ) per inspired oxygen fraction ( $\text{FiO}_2$ ) [20]. It remains under discussion whether machine perfusion techniques during transportation of the allograft and the corresponding limitation of the anoxic phase may blunt ischemia/reperfusion injury after transplantation and thereby improve postoperative outcomes [21]. There are some indicator suggesting that such techniques may reduce the incidence of post-transplant PGD. This however, may not impact on long-term outcomes [22].

#### *Pathophysiologic aspects*

The absence of nutritive arterial perfusion with oxygenated blood during ischemia leads to a depression of mitochondrial energy production and a depletion of adenosine triphosphate. This affects the intracellular ion homeostasis and cellular membrane permeability. Cellular necrosis and activation of apoptotic cell signals may

follow [23]. In addition, the fall in cellular energy content activates self-propagating deleterious cascades [23]. It is directly related to the production of reactive oxygen species (ROS) and reactive nitrogen species (RNS). Their production is induced during ischemia [24] and will increase rapidly during reperfusion [25]. Among all the potential sources and the formation pathways of ROS and RNS within cells, xanthine oxidases, nicotinamide adenine dinucleotide phosphate (NADPH) oxidases, and nitric oxide synthases (NOS) have been investigated [26].

Reperfusion of a transplanted allograft starts with the release of blood flow from the donor pulmonary trunc, passing the pulmonary arterial anastomosis into the grafts' pulmonary arterial vascular tree. The start of reperfusion is the restoration of blood flow in a previously anoxic graft, but it is at the same time the onset of microvascular perfusion failure within the grafted tissue [6]. The so-called "no reflow phenomenon" exacerbates hypoxia/anoxia in the grafted tissue despite the macroscopic restitution of the grafts blood circulation. The phenomenon describes the post-ischemic collapse of the graft's microcirculation due to endothelial cell swelling, hemoconcentration, narrowing of nutritive capillaries and interstitial edema formation [27-30]. Ischemia/reperfusion injury of a transplanted graft is an inflammatory response, an unspecific reaction rather than a cognitive response. The inflammatory response during ischemia reperfusion is a sterile process, which is activated by sterile cell death or injury. It has been confirmed that receptors, such as Toll-like receptors (TLRs) and DAPMs play a central roles in such immune response [31, 32]. When ligands bind to TLRs, cell signal pathways, such as NF-kB, mitogen-activated protein kinase (MAPK) and type I interferon pathways are activated, leading to the formation of pro-inflammatory mediators, such as cytokines and chemokines [33]. Neutrophils, monocytes and macrophages exert complementary functions during inflammation, also in the lung [34]. It is thought that, after stimulation, tissue resident macrophages and sentinel monocytes release chemokines and pro-inflammatory cytokines to recruit circulating white blood cells, primarily polymorphonuclear leukocytes, into the inflamed tissue compartment. Neutrophil infiltration and granule release is followed by monocyte recruitment in a secondary phase.

The early activation of alveolar macrophages via TLR-4 is thought to play a critical role in the development of lung ischemia/reperfusion injury [35, 36]. It has been shown that there was a significant increase in the number of alveolar macrophages

in bronchi-alveolar lavage fluid (BALF) after one hour hypoxia [37]. Using a murine lung transplantation model, it was shown that depletion of donor macrophages attenuated ischemia/reperfusion injury [38]. Suppressing of TLR-4 signalling inhibited the activation of alveolar macrophage as well and lung ischemia/reperfusion injury was almost completely attenuated [39]. Due to oxidative stress, alveolar macrophages produce monocyte chemoattractant protein-1 (MCP-1) and macrophage inflammatory protein-2 (MIP-2) which contribute to infiltration of neutrophils and lead to pulmonary oedema [40]. Beside this, macrophages can release tumour necrosis factor- $\alpha$  (TNF- $\alpha$ ), one of the pro-inflammation cytokines which can lead to acute lung damage directly [41]. In a rabbit lung ischemia/reperfusion injury model, TNF- $\alpha$  rose continuously during reperfusion and by attenuation TNF- $\alpha$ , the alveolar cell apoptosis and acute lung injury could be inhibited [42].

Also monocytes have been suggested to be involved in pulmonary ischemia/reperfusion injury. Classical monocytes are considered to be pro-inflammatory, since they can produce pro-inflammatory cytokines and differentiate into macrophages and dendritic cells [43]. In a model of lung ischemia/reperfusion injury, classical monocytes were found to be mobilized from their natural reservoir in the spleen, to enter into pulmonary tissue and provoke subsequent neutrophilic infiltration into the lung by releasing IL-1 $\beta$  [44]. Non-classical monocytes are thought to regulate wound healing and the resolution of inflammation. As such, they may be important mediators in lung injury as well. It was shown in a murine lung transplantation model that the depletion of donor intravascular non-classical monocytes, both pharmacologically and genetically, attenuated lung graft injury [45]. However, the precise role of non-classical monocytes, particularly in lung ischemia/reperfusion injury is still unclear [44].

The recruitment of circulating polymorphonuclear leukocytes (PMNLs), i.e. neutrophils, is a paramount feature of ischemia/reperfusion injury. This has been studied extensively in various organs such as the liver, striated muscle, intestine, kidney and the heart [46-49].

There has been conflicting data on the role of neutrophils in pulmonary ischemia/reperfusion injury. Neutrophils were initially thought to be unnecessary in lung ischemia/reperfusion injury [50, 51]. However, it was postulated that lung

ischemia/reperfusion injury has distinct phases [52, 53]. There seems to be an early phase, which is independent of neutrophils, while neutrophilic infiltration occurs later and is associated with increased pulmonary vascular permeability. Obviously, the activation of the pulmonary microvascular endothelium is a crucial part for the recruitment of neutrophils during lung ischemia/reperfusion injury. It is induced by TNF- $\alpha$ , IL-1 $\beta$  and will lead to an up-regulation of certain adhesion molecules on the luminal surface of the pulmonary vascular endothelium [54]. The recruitment of blood-borne white blood cells into the lung has been suggested to follow the same pattern of neutrophil recruitment in other organs (Figure 2). Neutrophils are thought to roll along the activated pulmonary endothelial surface orchestrated by a cytokine gradient and mediated by adhesion molecules of the selectin family, i.e. P- and/or L-selectin on neutrophils binding to E-selectin on the pulmonary endothelial surface. Further activation of the rolling cell will slow it down and more firm attachment is then mediated by the integrin family of adhesion molecules. The final step is the transendothelial migration. It is unknown, however, whether the transmigrating cell passes the endothelial lining between or directly through the endothelial cells [54]. The number of infiltrated neutrophils correlates to the severity of tissue damage [55]. By reducing the alveolar infiltration of neutrophils in a rat lung transplantation model, the gas exchange after surgery was improved [56]. It was thought that neutrophils exert lung ischemia/reperfusion injury by releasing elastase and granular proteins [57]. Neutrophil extracellular trap is an extracellular complex, including DNA, histones and neutrophil granular proteins [58]. Cadrillier et al found that neutrophil extracellular traps were created during lung transfusion and related to acute lung injury [59]. It was further shown that the neutrophil extracellular traps accumulated and contribute to primary graft dysfunction after lung transplantation as well [60].

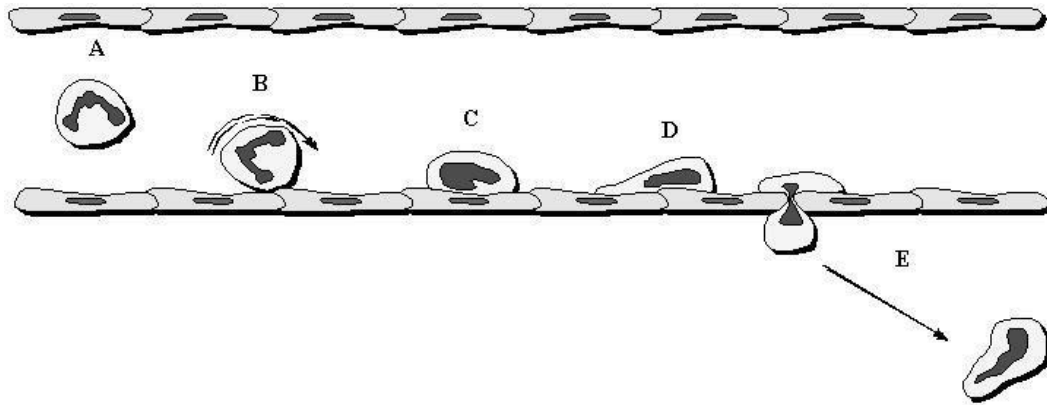


**Figure 2:** Schematic sequence of leukocyte recruitment in a microvessel. The extravasation of circulating leukocytes during inflammation may be defined as a sequential cascade of events including (A) free flowing, B) rolling, C) activation, D) firm adhesion and, finally, E) transmigration of inflammatory cells. Blood flow is from left to right. (The use of this figure has kindly been granted by Rene Schramm, Heart and Diabetes Center NRW, Bad Oeynhausen, Germany)

Despite these lines of evidence strongly suggesting that circulating leukocyte recruitment from the pulmonary vasculature is a key feature in lung ischemia/reperfusion injury, it has to be noted that the underlying evidence has been gathered only indirectly. Direct visualization of the pulmonary microvasculature during reperfusion has not been performed. It has to be considered also that the so-called marginated pool of leukocytes, i.e. a large number of granulocytes residing in the lung under normal physiological conditions, may have affected the results of previous studies [61-63].

Ischemia/reperfusion injury can affect platelet function and the coagulation system due to ROS induced increases in extracellular adenosine di-phosphate concentrations and endothelial cell injury induced activation of the von Willebrand factor (vWF) and thrombin [64-66]. Activated platelets may also interact directly with endothelial cells via selectins, which has been shown to cause microvascular constriction, aggravate postischemic injury and lead to thrombus formation [10]. P-selection can regulate platelet-endothelium interaction and promote platelet-leukocyte interaction during ischemia/reperfusion injury [67]. Finally, activated platelets form microthrombi perpetuating endothelial cell injury and microvascular dysfunction [68].

Microvascular permeability is increased because of hypoxia during reperfusion, triggered by the rapid production of ROS, complement activation, leucocyte-endothelial cell adhesion and platelet-leucocyte aggregation [6, 69]. In lungs, it presents as the alveolar-capillary barrier dysfunction which can lead to pulmonary edema and ultimately induces respiratory failure [70]. Vascular endothelial growth factor and angiopoietin-2 are considered as mediators of vascular permeability in lung ischemia/reperfusion injury [71, 72]. Several approaches may attenuate this alveolar-capillary dysfunction. For example, dimethylthiourea reduces postischemic microvascular dysfunction via its hydroxyl radical scavenger effects [73]. Hypoxia-inducible factor 1 $\alpha$  (HIF-1 $\alpha$ ) controls endothelial function, but is downregulated in lung ischemia reperfusion injury. Stabilizing it can prevent endothelial dysfunction [74]. Sphingosine 1-phosphate (S1P) controls endothelial cell tight junctions and supplementation with this compound before reperfusion inhibits inflammatory cytokine production and improves oxygenation in murine lung ischemia/reperfusion [75]. Antibody targeting of  $\alpha v\beta 5$ , an integrins that regulates endothelial permeability, also improved the postischemic oxygenation in a murine lung transplantation model [76].

### **3.3. Intravital fluorescence microscopy (IVM)**

The principle of fluorescence microscopy is that a distinct fluorescent dye can be rayed with light of a defined wavelength (excitation wavelength) and in response emits a quantum of light with a corresponding, different wavelength (emission wavelength) (Figure 3). This phenomenon is based on the fact that the excitation light transports energy. Distinct electrons on the fluorescent dye molecule adsorb photons and are thereby lifted to another energy level. This is an unstable condition and these electrons fall back into their original, lower energetic level immediately. This fall back liberates another quantum of energy, which is emitted as light. Because the liberated energy content is somewhat smaller, the emitted light quantum has a longer wavelength.

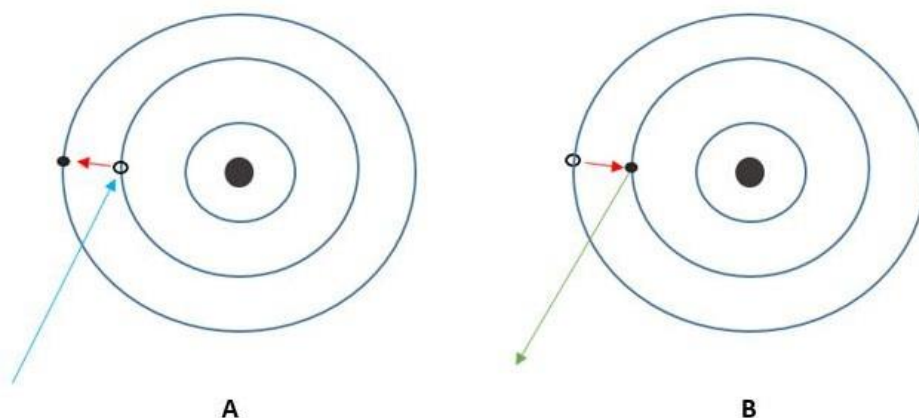


**Figure 3:** Schematic illustration of the excitation of a fluorescent dye on the atomic level. The schematic images show a molecule with a central atomic nucleus (large central black spot) encircled by three electron energy levels (blue circles). **A)** depicts the excitation of a resting electron on the second level (open spot) with fluorescent blue light. The concomitant energy transfer lifts the electron up to a higher energy level (filled spot). **B)** depicts the fact that the electron immediately loses this additional energy, falls back to a lower level and the originating slightly lower energy is emitted as fluorescent green light.

Epi-illumination microscopy uses filter sets, which allow to differentiate between excitation and emission light (Figure 4). The light source (herein a mercury lamp) of the microscope emits light through an excitation filter, which absorbs the wide spectrum of light letting pass exclusively light of the defined excitation wave length. This virtually single-coloured light hits onto the fluorescent dye and provokes the emission of lower energetic excitation light, which is reflected back to a filter letting pass only light of the defined excitation wavelength. Reflected light of the excitation wavelength is absorbed. The resulting image is constructed of the residual emitted light.

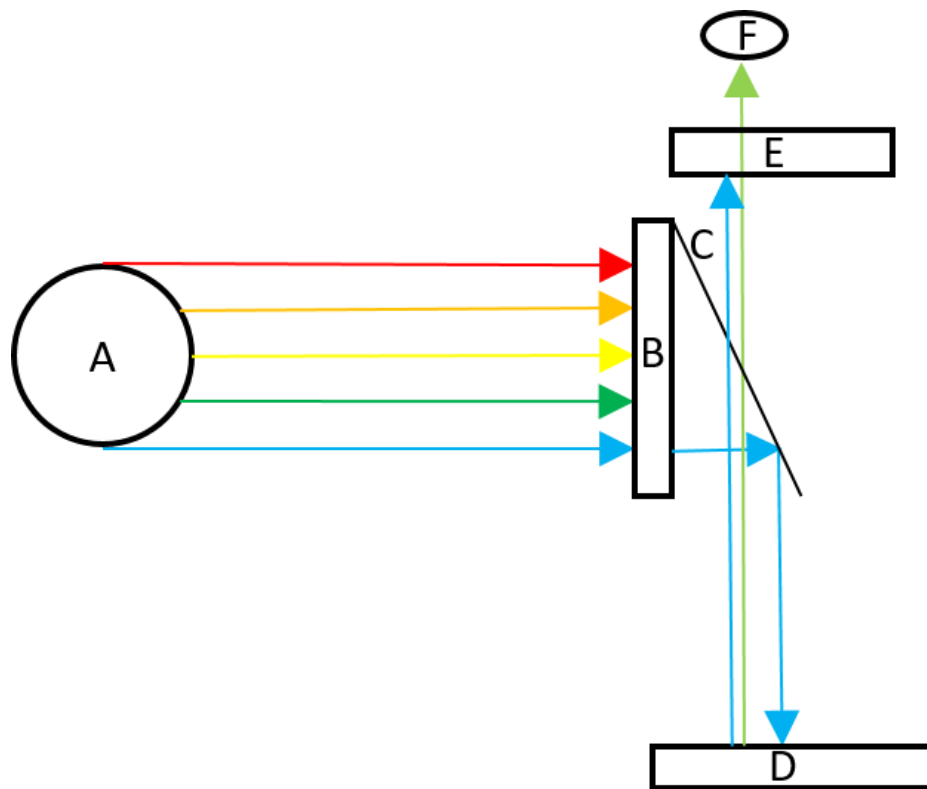


**Figure 4:** Schematic illustration of the principle of an epi-illumination fluorescence microscope. A: Light source; B: Filter for Excitation light; C: Beam splitter; D: Experiment object with fluorescent dye; E: Filter for Emission light; F: Camera

*IVM in experimental research on ischemia/reperfusion injury*

IVM has been utilized for the analyses of cell-cell interactions and microvascular dysfunction in a large array of experimental models. The use of this technique has allowed to understand the stepwise mechanisms of the leukocyte extravasation process during inflammation. For example, in hepatic injury, selectin-mediated leukocyte rolling was found to be a prerequisite for subsequent integrin-mediated firm adhesion of leukocytes [77]. Such fundamental and distinct roles of P-selectin and the integrin lymphocyte function associated antigen (LFA)-1 were directly visualized during in the postischemic microcirculation of the murine colon [78]. Postischemic vasoreactivity could be demonstrated in in the intestinal microcirculation as well [29]. In the murine striated cremaster muscle preparation, it was demonstrated

that chemokines regulate selectin-dependent neutrophil trafficking in a mast cell-controlled manner [79].

IVM of the thoracic organ microcirculation has been challenging, since tremendous physiologic movements elicited by the beating heart and the ventilated lungs have to be counterbalanced. Nevertheless, distinct experimental models have been elaborated to circumvent such hurdles and both the subepicardial coronary microcirculation of the heart and the subpleural pulmonary microcirculation of the lung could be visualized even in small animals as the mouse [80, 81]. In both latter organs, the sequential leukocyte extravasation cascade has been visualized. However, pulmonary ischemia/reperfusion injury has not been investigated so far by IVM in a rodent model.

#### **4. Aim of the study**

Detailed understanding of the pathophysiological mechanisms underlying pulmonary ischemia/reperfusion injury are key to improve outcomes after lung transplantation clinically. Although circulating white blood cell recruitment and microvascular dysfunction during pulmonary ischemia/reperfusion injury have been investigated previously, evidence on the underlying mechanisms have been gathered mostly indirectly, experimentally and clinically. Further, results obtained from cell cultures and isolated organ perfusion experiments may not resemble the complex interplay of pathophysiological processes as in a live individual.

The aim of the present study was it therefore to establish and validate an experimental approach which allows to study leukocyte recruitment and microvascular dysfunction within the pulmonary microcirculation during ischemia/reperfusion injury in a rodent model by means of intravital fluorescence microscopy. The experimental setup should also allow to monitor potential secondary organ dysfunction in the heart, liver and kidney by histopathological means. The experimental setup should be reproducible and provide an experimental basis for studies on experimental lung transplantation.

## **5. Materials and Methods**

### **5.1. Animals**

Female Lewis rats (Charles River) weighing 220-240g were used. The animals had free access to standard pellet food and tap water and were kept in 12h light and 12h dark cycles. All experiments were approved by the governmental ethical committee for animal experimentation and performed as the legislation on the protection of animals. Animals were sacrificed immediately after the experiment in deep anaesthesia through exsanguination.

### **5.2. Experimental procedures**

#### **5.2.1. Anesthesia**

Global anaesthesia was induced by intramuscular injection of a mixture of medetomidine (150 µg/kg body weight, Domitor), midazolam (2 mg /kg body weight, Dormicum) and fentanyl (5 µg/kg body weight, Fentanyl-Janssen) into the right quadriceps femoris muscle.

The anesthetized animals were placed in a supine position for subsequent endotracheal intubation with a 16G catheter (Introcan Safety, Braun Melsungen AG, Melsungen, Germany) under direct vision. The catheter was then connected to small animal ventilator (Small animal ventilator KTR-5, Harvard Apparatus, Canada). Correct endotracheal intubation was additionally verified by synchronic expansion of the thoracic cage. The basic settings for the ventilator were settled to 75 strokes per minute with an inspiration/expiration ratio of 1 / 2. The air flow was adjusted to 0.5 liters / min with a positive end-expiratory pressure of 9 cm H<sub>2</sub>O without additional oxygen supply. The respirator settings were adjusted throughout the experimentations based on arterial blood gas analyses.

Central catheter implantation was performed as previously described [82]. Briefly, after intubation, an incision was made on the right paramedian aspect of the neck. of the rat, then the right external jugular vein and the right common carotid artery were exposed gently. The two vessels were secured proximally and distally by ordinary silk ordinary silk suture. Two central 20G catheters (BD Microlance, Becton Dickinson

S.A. Fraga, Huesca, Spain) were then inserted into the two vessels, flushed with saline and secured by the silk sutures (Figure 5).

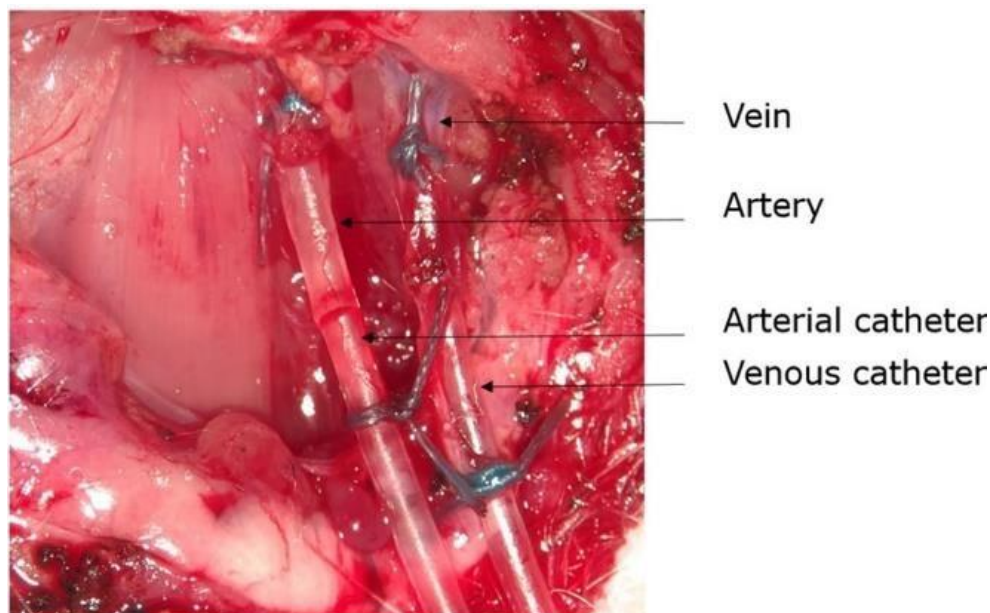


**Figure 5:** Central catheterization of the right jugular vein and common carotid artery.

### 2.2.2 Microsurgical procedures

The lateral thoracotomy approach to the lung has been described in a murine model previously by Gielis et al [83]. After placement of the animal from the supine into the right lateral position, the chest wall was shaved gently. The incision was made beginning at the medial sternal side of the left rib cage and was followed along the 5<sup>th</sup> intercostal space directed to the spine. After disconnecting the endotracheal tube from the respirator, great care was taken when blunt penetration of the intercostal muscular layer was performed in order to avoid any alteration of the visceral pleural surface of the lung. Respiration was continued immediately after the thoracic cavity has been opened safely. The rib cage was spread open by placing two 1-0 holding sutures (Prolene, Polypropylen, Ethicon, USA) around the adjacent upper and lower ribs and pulling them gently towards the cranial and caudal directions. The lung tissue was moistened by temperature (37°C) saline regularly throughout the entire experimentation. A moistened cotton stick was used to gently move the pulmonary

tissue taking great care to not touch the ventral aspect of the lung, i.e. the region of interest for subsequent intravital fluorescence microscopy. The pulmonary ligament was cut off in order to get a better access to the lung hilum. Before clamping of the hilum for induction of ischemia, 125 I.U. of heparin (Rotexmedica, Trittau, Germany) was administered intravenously (i.v.). Clamping was performed by use of an ordinary microvascular vessel clamp (Figure 6). The lung and pleural cavity was kept moistened with temperature saline (37°C) throughout the entire experiments.

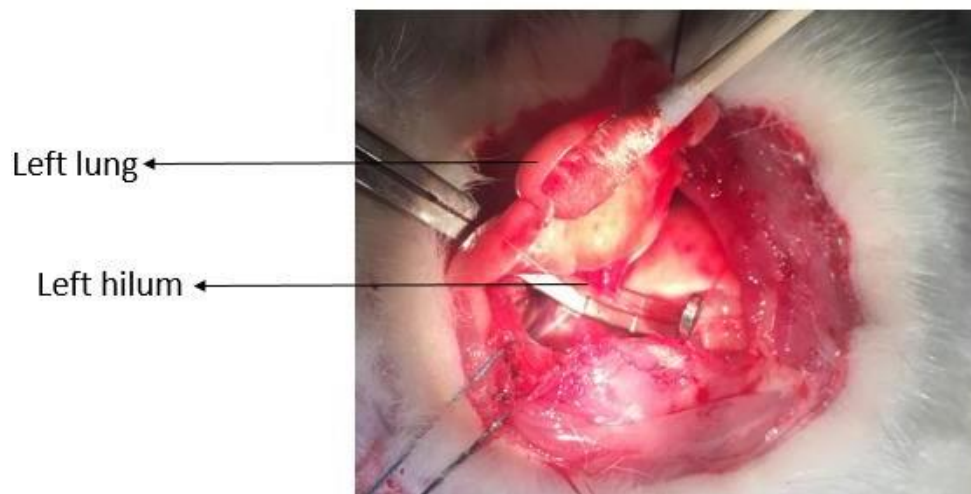


**Figure 6:** Macroscopic image of the surgical field during clamping of the left pulmonary hilum, i.e. during ischemia.

### **5.3. Intravital fluorescence microscopy**

#### **5.3.1. Imaging**

The microsurgically equipped and prepared animals were transferred to the intravital microscope stage. Intravital fluorescence labelling of circulating leukocytes was established by i.v. injection of 0.5 ml of Rhodamine 6G (Molecular weight 479 Da; 0.1 mg/ml, Sigma Chemicals). For plasma labelling, an injection of Fluoresceine Iso-Thyo-Cyanate (FITC)-Dextran (Molecular weight 150 kDa; 2 mg/ml, Sigma Chemicals) was injected via the central venous catheter. The moistened left lung surface was carefully covered with a horizontally positioned cover glass slip, which was fixed to a micromanipulator. The hydrostatic forces of the moistening saline attached the lung surface under the cover glass slip (Figure 7). The subpleural pulmonary

microcirculation of the left lung was visualized by a modified microscope (Zeiss, Oberkochen, Germany), which provides blue- (excitation wave length 490nm) and green-light (excitation wavelength 530nm) epi-illumination and is equipped with a filter set (Filter set 62HE, Colibri, Zeiss, Germany) to visualize the corresponding emission wave lengths of 510nm and 560nm, respectively. Water immersion lenses with a 10- and 20-fold magnification were used. All microscopic images were televised and recorded onto a computer-assisted hard disc drive.

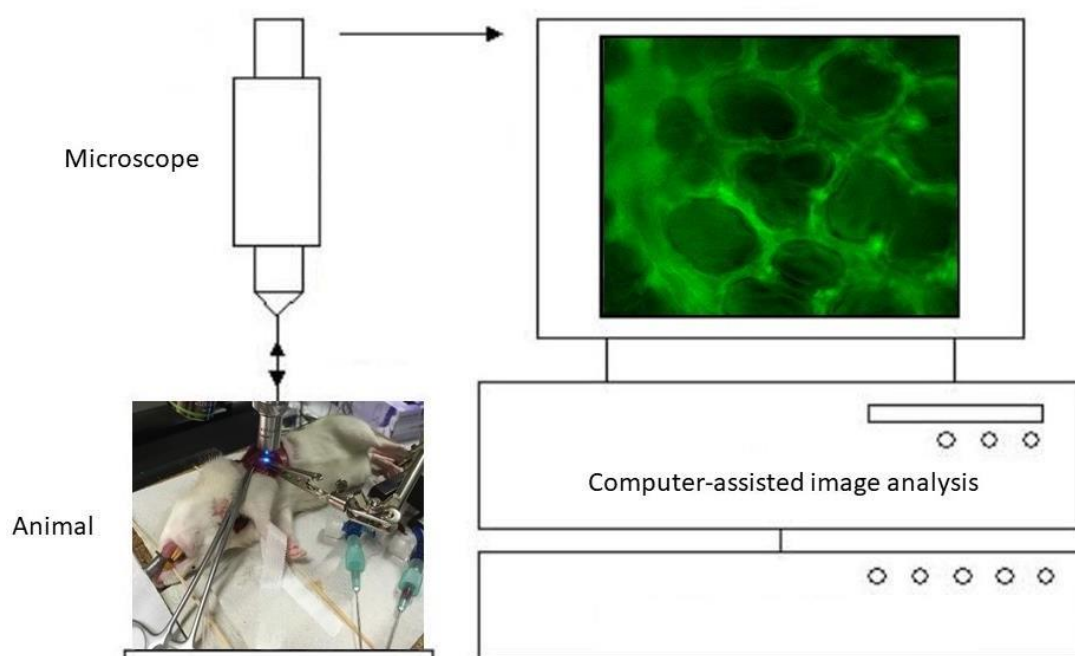


**Figure 7:** Schematic experimental setup for intravital fluorescence microscopy (IVM) of the rat pulmonary microcirculation. Animals were placed in a right-sided position on the microscope stage. Microscopic images were transferred to a computer-assisted image analysis system and saved onto a hard disc for subsequent off-line quantification of experimental parameters.

### 5.3.2. Parameters

Intravital fluorescence microscopy of the left lung subpleural pulmonary microcirculation was performed at three different time points, i.e. before induction of ischemia (T0), at 30min of Reperfusion (T1) and after 90 min of reperfusion (T2). At

least four different areas were analysed at each individual time point for at least 30 seconds.

#### *Leukocyte endothelial cell adhesive interactions*

Firm leukocyte adhesion was defined as the number of intravascular leukocytes firmly attached for >15 seconds to the pulmonary microvascular endothelial cell lining of pulmonary arterioles and venules, given in cells / mm<sup>2</sup> endothelial surface. Leukocyte rolling was defined as the number of intravascular leukocytes loosely interacting with and rolling along the endothelial lining passing a reference point within pulmonary arterioles and venules during the observation period of 30 seconds, given in cells / min.

#### *Alveolar leukocyte recruitment*

The numbers of Rhodamine 6G-stained leukocytes within alveolar spaces were counted and are given as cells per high power field (HPF) [aU].

#### *Macromolecular leakage*

The extravascular fluorescence intensity was measured within alveolar spaces after intravenous injection of the fluorescent dye FITC-dextrane at T0, T1, and T2. To account for different animal body weights and circulating blood volumes the individual measures at T1 and T2 were normalized by the intra-individual measurements at T0.

#### *Distance of air-filled alveolar spaces*

The distance of air-filled alveolar spaces is an indirect measure for interstitial pulmonary edema formation and is given in  $\mu\text{m}$ .

#### *Microvascular diameters*

The diameters of pulmonary terminal arterioles, alveolar capillaries and draining postcapillary venules are given in  $\mu\text{m}$ .

### **3.4. Histopathological analyses**

After completion of the experimental procedures and intravital microscopic analyses, i.e. after 90 min of pulmonary reperfusion (T2), both lungs, the heart, the kidneys and the livers were harvested for subsequent histopathological examination. The lungs were harvested by ligation and transection in inspiration. The other organs were harvested by transection of incoming and outgoing vessels. All organs were fixed in 4% paraformaldehyde overnight and were then stored in 80% ethanol until further processing.

For routine hematoxylin-eosin staining, organ tissues were dehydrated in an ascending concentration of ethanol series and the ethanol was removed by aromatic hydrocarbon xylene. Afterwards all organs were embedded in paraffin wax and cut into 4 µm thick layers with a microtome (Leica Biosystems, Germany) and fixed on a glass slide. The sections on the glass slips were dewaxed in a descending concentration of ethanol series and stained by haematoxylin and eosin in an ascending concentration of ethanol series. The basophilic structures were stained blue with haematoxylin, the acidophilic structures were stained red with eosin.

The evaluation of the histological specimens were carried out by use of a light microscope (Zeiss, Oberkochen, Germany), which was connected to a digital camera (Zeiss, Oberkochen, Germany) and a corresponding computer-assisted software, the Axiovision (Zeiss, Oberkochen, Germany). 25 fields per slide were evaluated in each organ in 200× high-power-fields (HPFs).

Pulmonary injury was semi-quantitatively analysed by using a lung injury score system, previously published by the American Thoracic Society Workshop [84] (Table 1). Secondary organ damage to the kidney and liver were analysed quantifying the areas of tubular necrosis per HPF [85] and by use of the previously published Suzuki Score system (Table 2) [86], respectively.

Parameter	Score per field		
	0	1	2
A. Neutrophils in the alveolar space	None	1-5	>5
B. Neutrophils in the interstitial space	None	1-5	>5
C. Hyaline membranes	None	1	>1
D. Proteinaceous debris in the air space	None	1	>1
E. Alveolar septal thickening	<2x	2x – 4x	>4x

Final score= [(20 × A) + (14 × B) + (7 × C) + (7 × D) + (2 × E)]/( number of fields × 100)

**Table 1:** The Lung Damage Score for quantification of structural pulmonary injury. Adopted from [84].

Score	Congestion	Vacuolization	Necrosis
0	None	None	None
1	Minimal	Minimal	Minimal
2	Mild	Mild	Mild
3	Moderate	Moderate	Moderate
4	Severe	Severe	Severe

The level of damage was defined by planimetry in each high power field. Minimal = 0 - 10%, Mild= 11% - 30%, Moderate= 31% -60%, Severe= over 61%

**Table 2:** The Suzuki Score system for quantification of structural liver injury. Adopted from [86].

## **5.5. Statistical analysis**

Data are given as mean values  $\pm$  standard error of the mean (SEM) and n represents the number of animals per experimental group and/or time point. Data was analysed using one-way analyses of variance (ANOVA) and corresponding post-hoc testing utilizing statistic computer software packages (SPSS 22, IBM, USA; SigmaStat, Jandel Scientific, USA). A value of probability of less than 0.05 was considered to indicate a statistically significant difference.

## **6. Results**

### **6.1. Intravital fluorescence microscopic imaging (IVM)**

During the learning curve, six animal preparations did not allow for the planned IVM observations. These animals had to be sacrificed because of technical failure, uncontrolled respiratory acidosis or insufficient exposure for intravital imaging. In a total of 8 animals, successful surgical preparation was followed by intravital fluorescence microscopic observation (IVM) of the pulmonary microcirculation before ischemia and at 30 min (T1) as well as 90 min of reperfusion (T2).

The entire pulmonary microvascular tree could be visualized after contrast enhancement with FITC-Dextran including feeding pulmonary arterioles, alveolar capillaries and draining pulmonary venules (Figures 8-10). Pulmonary arterioles were differentiated from venules by the peripheral branching of blood flow and visible pulsatility. Venules were draining the blood from peripheral branches and did not show any pulsatility. Bronchial arteries could not be differentiated.

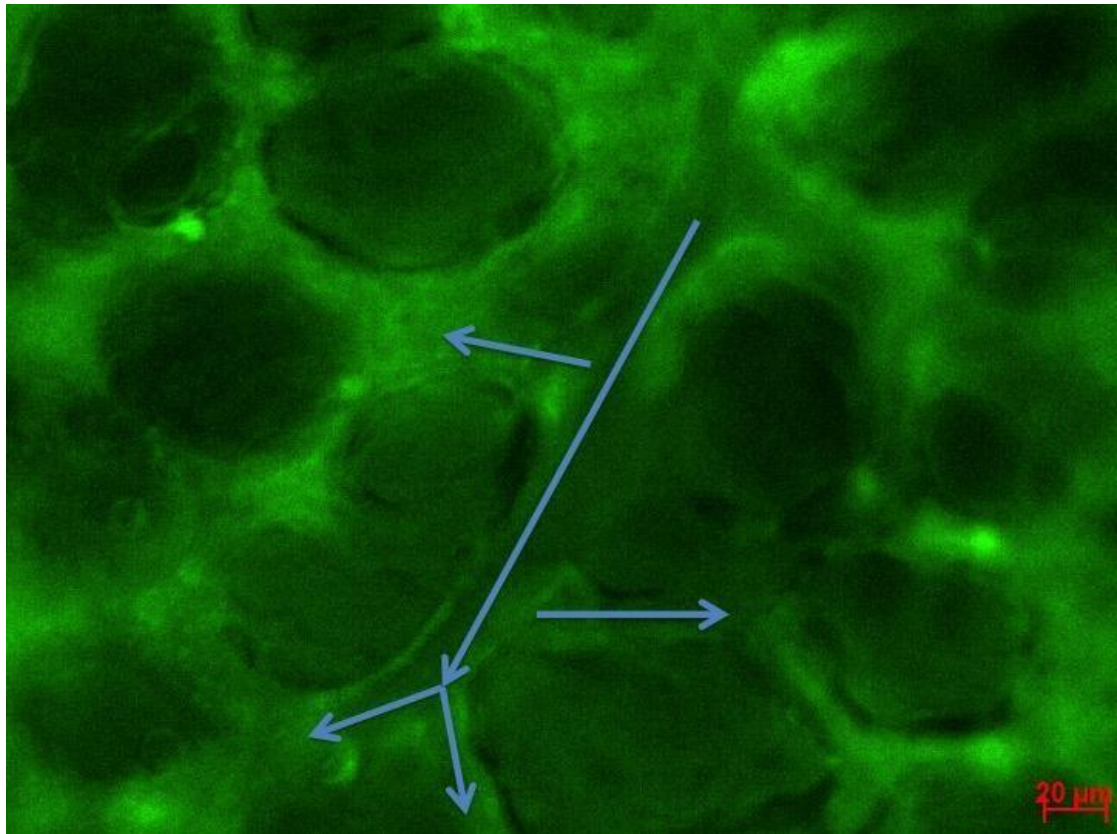


**Figure 8:** Intravital microscopic image of the pulmonary microcirculation in the left lung upper lobe. Contrast enhancement after intravenous injection of FITC-Dextran at 90 min of reperfusion (T2). Blue arrows indicate the distributing and divergent blood flow of the central arteriole into alveolar capillaries. Scale represents 20 μm.

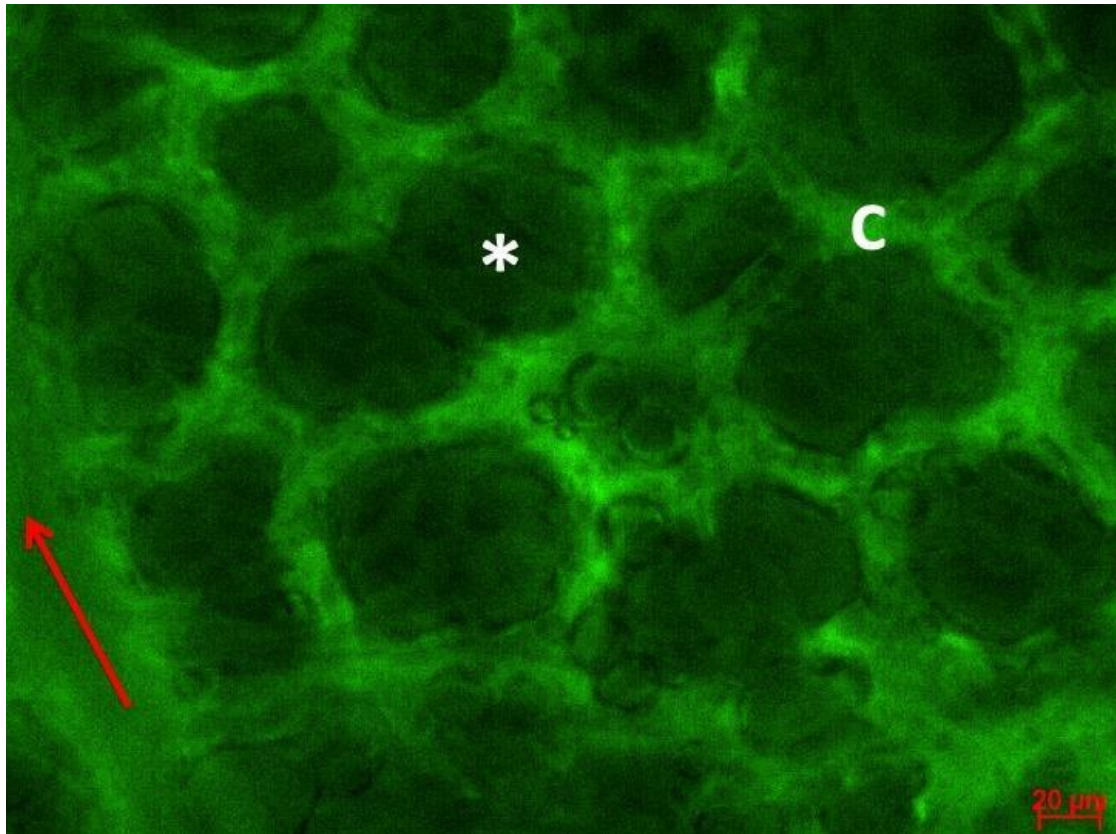


**Figure 9:** Intravital microscopic image of the pulmonary microcirculation in the left lung upper lobe. Contrast enhancement after intravenous injection of FITC-Dextran prior to induction of ischemia (T0). The asterisk indicates an exemplary alveolar space surrounded by alveolar capillaries indicated by “C”. The red arrows indicates the blood flow in a draining pulmonary venule. Scale represents 20  $\mu\text{m}$ .

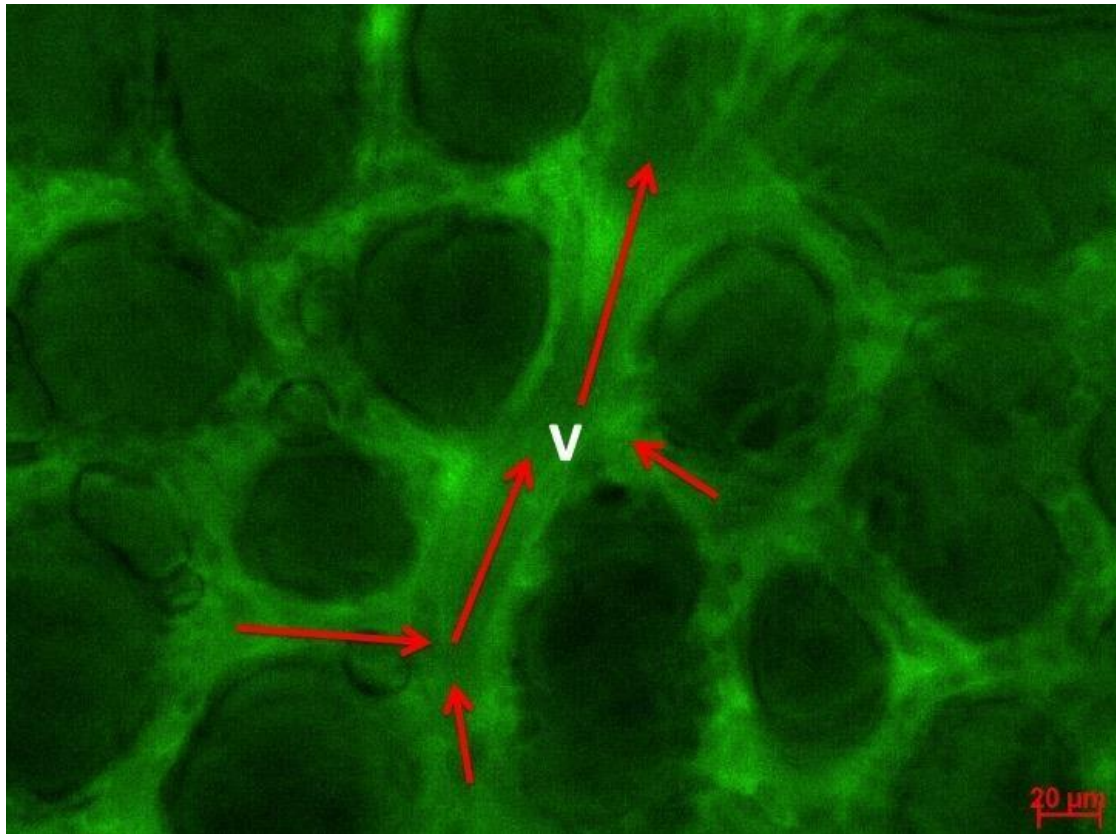


**Figure 10:** Intravital microscopic image of the pulmonary microcirculation in the left lung upper lobe. Contrast enhancement after intravenous injection of FITC-Dextran prior to induction of ischemia (T0). Red arrows indicate the collecting blood flow from alveolar capillaries into a draining venule (V). Scale represents 20 μm.

Contrast enhancement with Rhodamine-6G allowed to visualize intravascular leukocytes and occasionally thrombocytes. Leukocytes were differentiated from thrombocytes based on their size difference. Visualized leukocytes were presumably granulocytes as reflected by their irregularly and granulated nuclear staining (Figure 11).

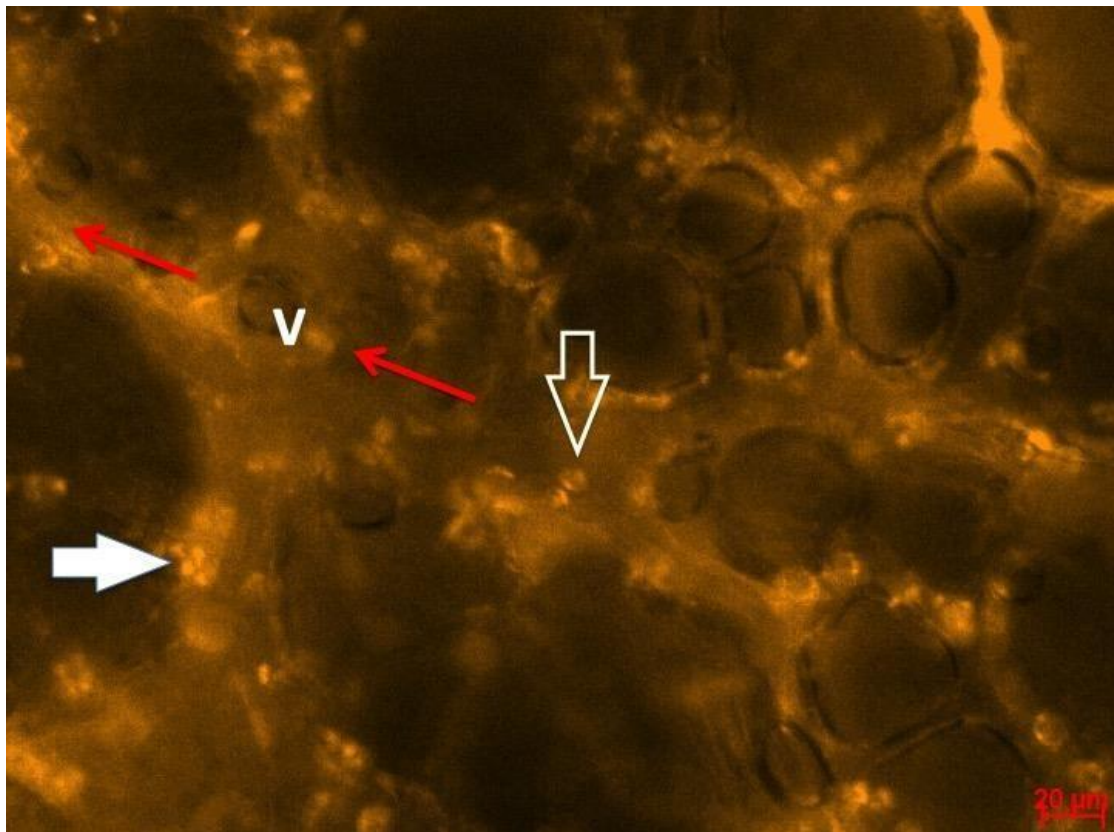


**Figure 11:** Intravital microscopic image of the pulmonary microcirculation in the left lung upper lobe. Contrast enhancement after intravenous injection of Rhodamine 6G at 90 min of reperfusion (T2). Red arrows indicate the collecting blood flow in a draining venule (V). The open arrow indicates an adherent leukocyte. The filled arrow indicates a group of intensely stained small thrombocytes. Scale represents 20  $\mu\text{m}$ .

## IVM – Parameters

### *Leukocyte endothelial cell adhesive interactions*

IVM allowed for quantitative and qualitative analyses of leukocyte endothelial-cell adhesive interactions in the pulmonary microcirculation of the left lung surface. Rhodamine-6G stained leukocytes were interacting with the pulmonary vascular endothelium only in post-capillary venules. Virtually no adhesive interactions were observed in arterioles at any time point. In addition, interacting leukocytes were found to be firmly attached to the post-capillary venular endothelium (Figure 11). Rolling interactions were just occasionally found.

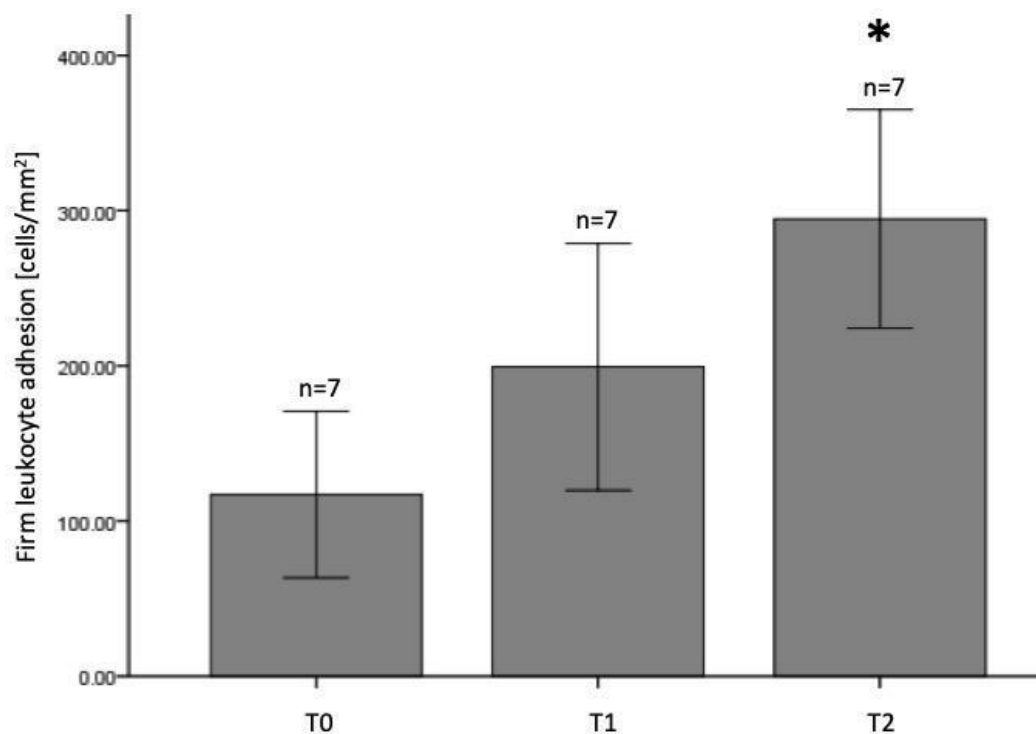


**Figure 12:** Firm leukocyte adhesion in post-capillary venules of the left lung pulmonary microcirculation. Data are given as mean values  $\pm$  standard error of the mean and n represents the number of animals at the different time points, i.e. prior to induction of ischemia (T0), at 30 min of reperfusion (T1) and at 90 min of reperfusion (T2). The asterisk indicates a statistically significant difference when compared to T0 ( $P < 0.05$ ).

Firm leukocyte adhesion was increasing from  $117.14 \pm 10.12$  cells/mm<sup>2</sup> at T0 (prior to induction of ischemia) to  $199.37 \pm 15.03$  cells/mm<sup>2</sup> at T1 (30min of reperfusion) and  $294.76 \pm 13.31$  cells/mm<sup>2</sup> at T2 (90 min of reperfusion). The difference between firm leukocyte adhesion at T0 and T2 was statistically significant (P=0.005; Figure 12).

#### *Alveolar leukocyte recruitment*

The numbers of Rhodamine-6G stained leukocytes within the alveolar spaces were  $1.88 \pm 0.17$  [aU] at T0 (prior to induction of ischemia),  $3.71 \pm 0.21$  [aU] at T1 (30min of reperfusion) and  $7.8 \pm 0.49$  [aU] at T2 (90 min of reperfusion). There were statistically significant differences between the alveolar space leukocyte counts between T0 and T2 (P=0.002) as well as between T1 and T2. (P=0.033; Figure 13).

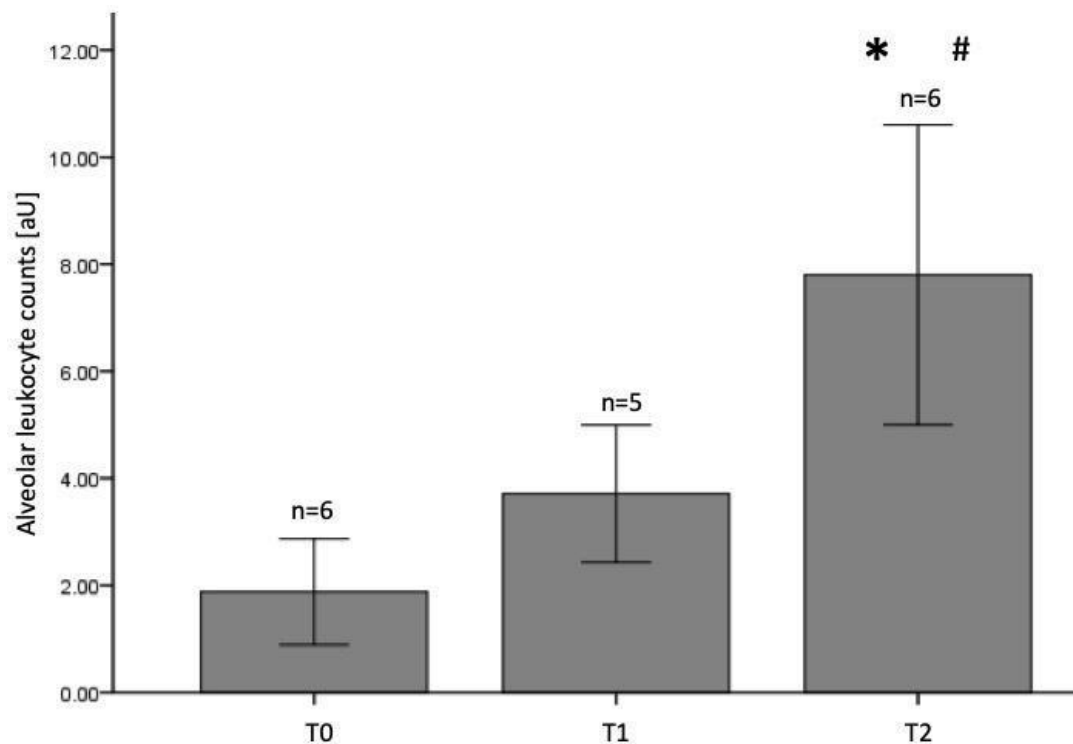


**Figure 13:** Numbers of leukocytes within alveolar spaces the left lung. Data are given as mean values  $\pm$  standard error of the mean and n represents the number of animals at the different time points, i.e. prior to induction of ischemia (T0), at 30 min of reperfusion (T1) and at 90 min of reperfusion (T2). \* indicates a statistically significant difference when compared to T0 (P<0.05). # indicates a statistically significant difference when compared to T1 (P<0.05).

### *Macromolecular leakage*

The extravascular fluorescence intensity was measured within alveolar spaces after intravenous injection of the fluorescent dye FITC-dextrane at T0, T1, and T2. To account for different animal body weights and circulating blood volumes the individual measures at T1 and T2 were normalized by the intra-individual measurements at T0. The T1/T0 and T2/T0 ratios were  $1.231 \pm 0.018$  [aU] and  $1.408 \pm 0.045$  [aU]. The difference between the ratios is statistically not significant ( $P=0.167$ ; Figure 14).

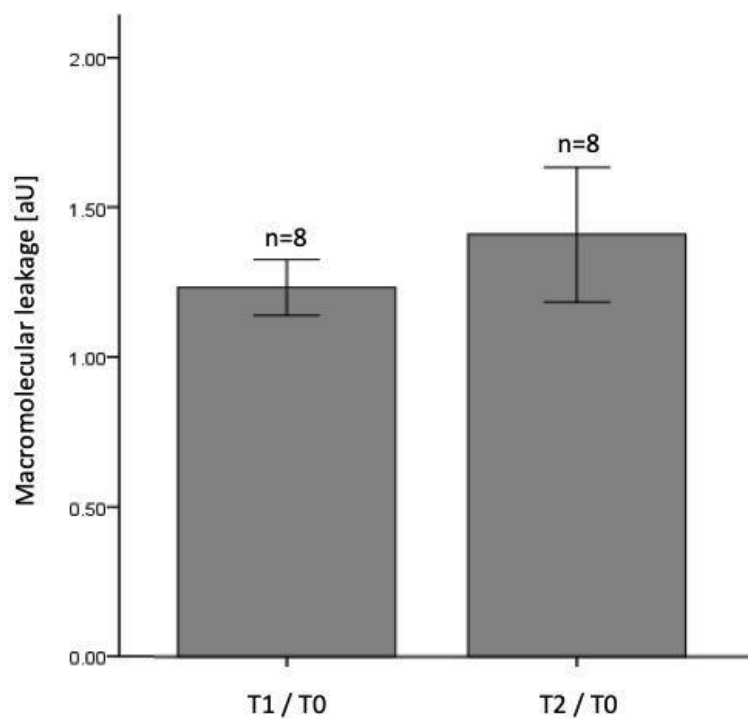


**Figure 14:** Macromolecular leakage in the left lung pulmonary microcirculation. To account for different animal body weights and circulating blood volumes the individual measurements of extravascular fluorescence intensity at T1 and T2 were normalized by the intra-individual measurements at T0. Data are given as mean values  $\pm$  standard error of the mean and n represents the number of animals at the different time points.

### *Distance of air-filled alveolar spaces*

The distance of air-filled alveolar spaces is an indirect measure for interstitial pulmonary edema formation. The mean distances between air-filled alveolar spaces were  $13.12 \pm 0.33 \mu\text{m}$  at T0,  $14.71 \pm 0.32 \mu\text{m}$  at T1 and  $15.78 \pm 0.29 \mu\text{m}$  at T2. The differences between the individual time points were statistically not significant ( $P=0.055$ ; Figure 15).

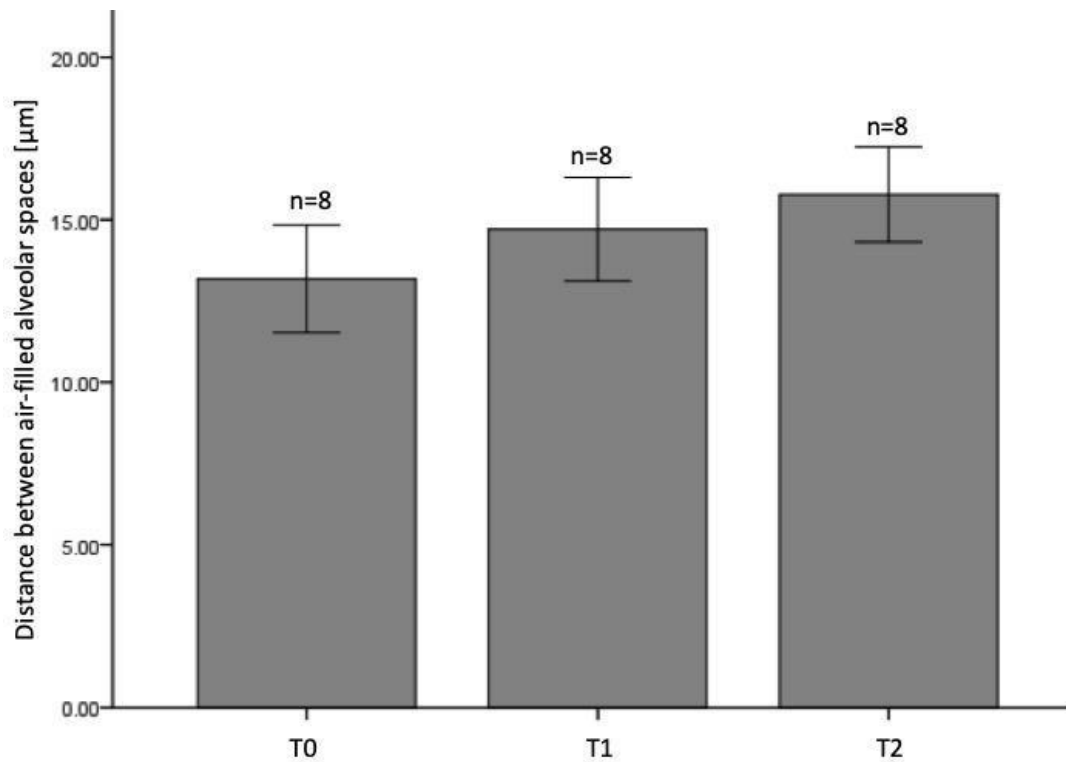


**Figure 15:** Distances between air-filled alveolar spaces given in  $\mu\text{m}$ . Data are given as mean values  $\pm$  standard error of the mean and n represents the number of animals at the different time points, i.e. prior to induction of ischemia (T0), at 30 min of reperfusion (T1) and at 90 min of reperfusion (T2).

### *Microvascular diameters*

The diameters of terminal pulmonary arterioles in the left lung surface, i.e. the final, capillary feeding arteriolar branches, did not relevantly change over the observation period. Arteriolar diameters were  $15.81 \pm 0.67 \mu\text{m}$  prior to induction of ischemia (T0),  $14.46 \pm 0.94 \mu\text{m}$  at 30 min of reperfusion (T1) and  $14.17 \pm 0.67 \mu\text{m}$  at 90 min of reperfusion (T2; Figure 16). The differences were statistically not significant.

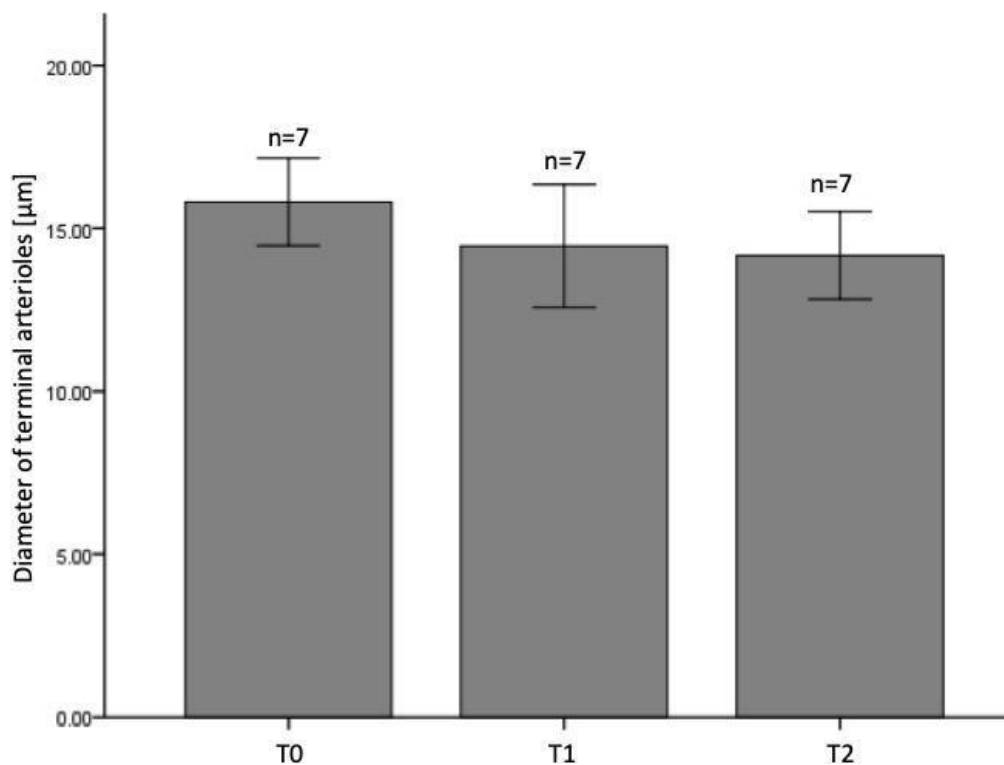


**Figure 16:** Diameters of terminal pulmonary arterioles. Data are given as mean values  $\pm$  standard error of the mean and n represents the number of animals at the different time points, i.e. prior to induction of ischemia (T0), at 30 min of reperfusion (T1) and at 90 min of reperfusion (T2).

In addition to terminal arterioles, the diameters of third grade arterioles, i.e. two bifurcations further upstream of terminal arterioles (Figure 17), were analysed. The mean diameters of third grade arterioles in the left lung surface did not relevantly change over the observation period. Mean diameters of third grade arterioles were  $23.78 \pm 2.63 \mu\text{m}$  prior to induction of ischemia (T0),  $21.96 \pm 1.28 \mu\text{m}$  at 30 min of reperfusion (T1) and  $19.61 \pm 1.70 \mu\text{m}$  at 90 min of reperfusion (T2; Figure 18). The differences were statistically not significant.

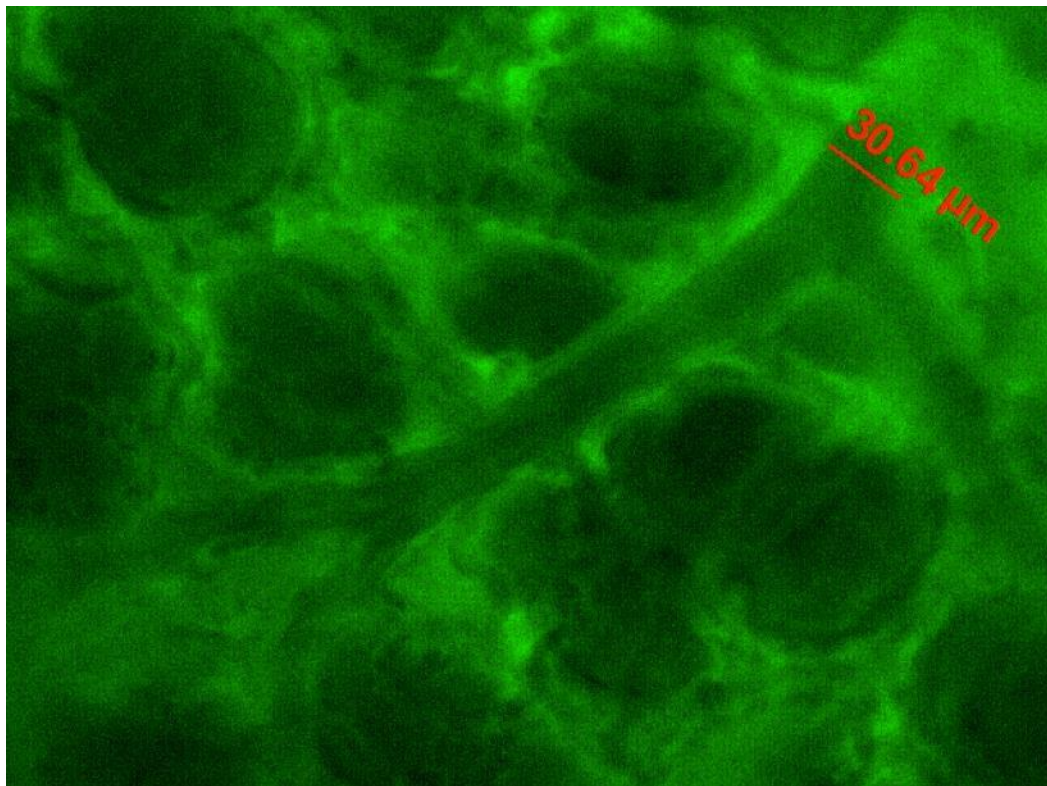


**Figure 17:** Intravital microscopic image of the pulmonary microcirculation in the left lung upper lobe. Contrast enhancement after intravenous injection of FITC-Dextran at 90 min of reperfusion (T2). The diameter of the central pulmonary arteriolar vessel is measured two bifurcations upstream the capillary branching level, i.e. in third grade arterioles.

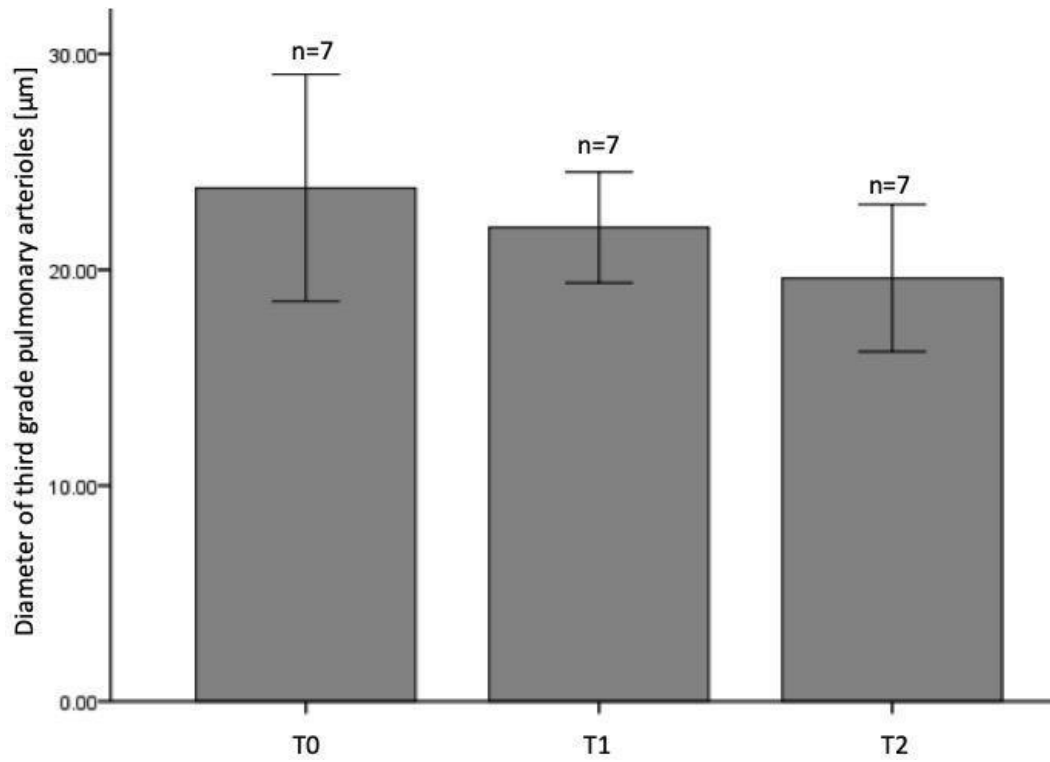


**Figure 18:** Diameters of third grade pulmonary arterioles. Data are given as mean values  $\pm$  standard error of the mean and n represents the number of animals at the different time points, i.e. prior to induction of ischemia (T0), at 30 min of reperfusion (T1) and at 90 min of reperfusion (T2).

The alveolar capillary diameter in the left lung surface did not relevantly change over the observation period. Mean diameters of pulmonary alveolar capillaries were  $5.30 \pm 0.13 \mu\text{m}$  prior to induction of ischemia (T0),  $5.72 \pm 0.18 \mu\text{m}$  at 30 min of reperfusion (T1) and  $5.63 \pm 0.11 \mu\text{m}$  at 90 min of reperfusion (T2; Figure 19). The differences were statistically not significant.

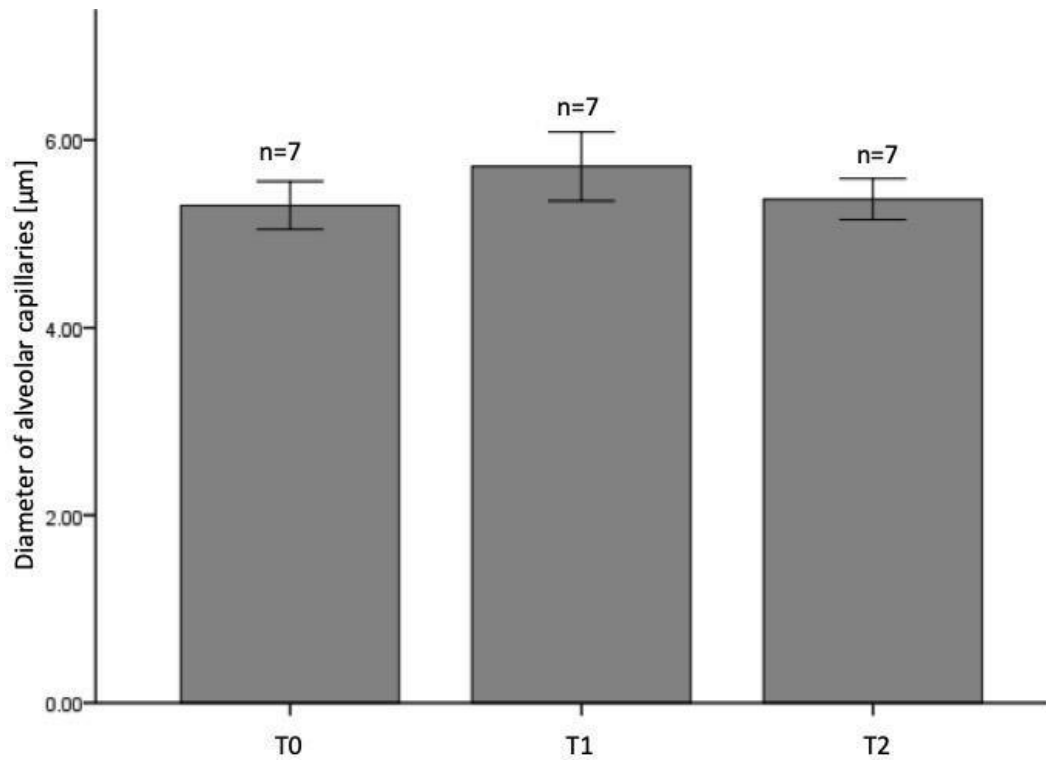


**Figure 19:** Diameters of alveolar capillaries. Data are given as mean values  $\pm$  standard error of the mean and n represents the number of animals at the different time points, i.e. prior to induction of ischemia (T0), at 30 min of reperfusion (T1) and at 90 min of reperfusion (T2).

The diameters of postcapillary pulmonary venules in the left lung surface did not relevantly change over the observation period. Postcapillary venular diameters were  $20.04 \pm 0.85 \mu\text{m}$  prior to induction of ischemia (T0),  $18.47 \pm 0.71 \mu\text{m}$  at 30 min of reperfusion (T1) and  $16.51 \pm 0.62 \mu\text{m}$  at 90 min of reperfusion (T2; Figure 20). The differences were statistically not significant.

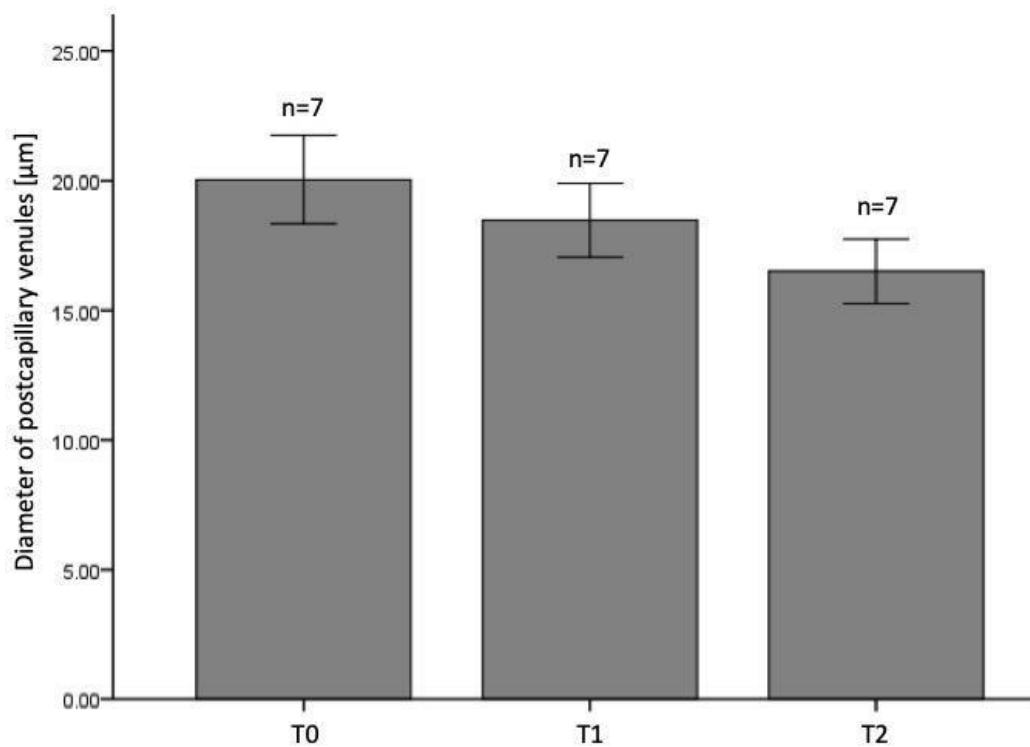


**Figure 20:** Diameters of post-capillary pulmonary venules. Data are given as mean values  $\pm$  standard error of the mean and n represents the number of animals at the different time points, i.e. prior to induction of ischemia (T0), at 30 min of reperfusion (T1) and at 90 min of reperfusion (T2).

## 6.2. Histopathologic analyses

### *Histopathology of the lungs*

The histopathologic analysis of lung tissue specimens harvested after 90 min of reperfusion (at T2), indicated mild damage to the pulmonary parenchymal tissue architecture. Figure 21 shows a high power field of a histopathologic specimen of a left lung harvested at T2 with mild alveolar septal thickening and some leukocytic infiltrations. As an internal control, Figure 22 shows a high power field of a histopathologic specimen of a right lung harvested at T2.

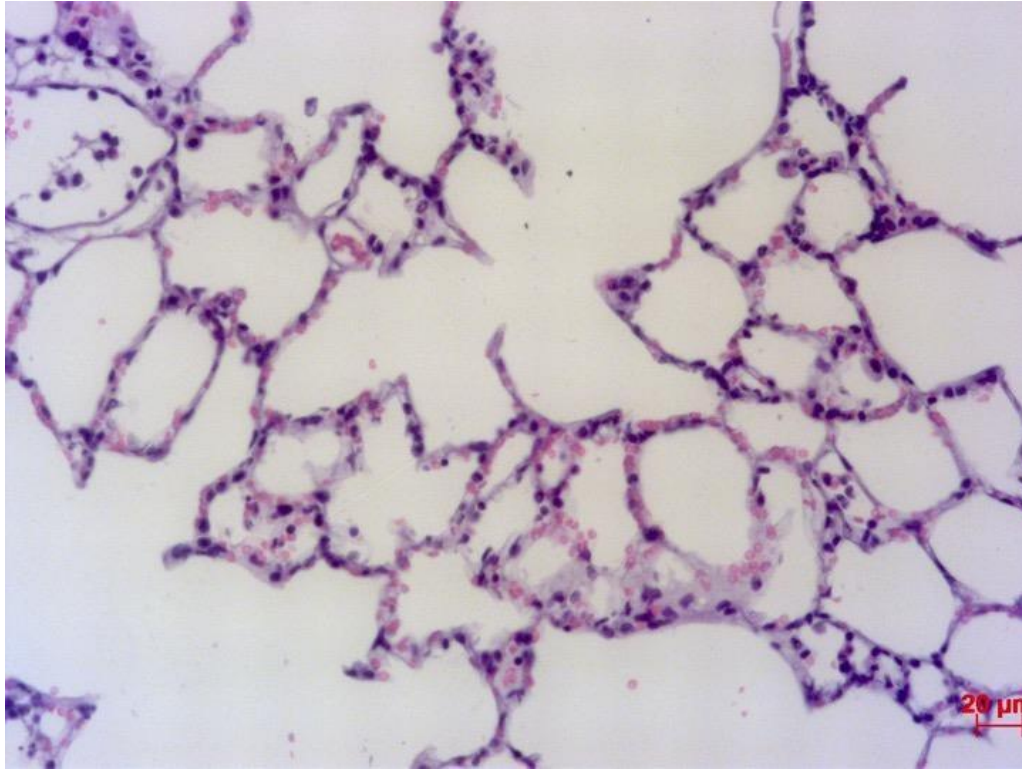


**Figure 21:** Exemplary histological specimen of a left lung, harvested after 90min of reperfusion (T2). Routine hematoxylin-eosin staining. Scale bar represents approximately 20 $\mu$ m.

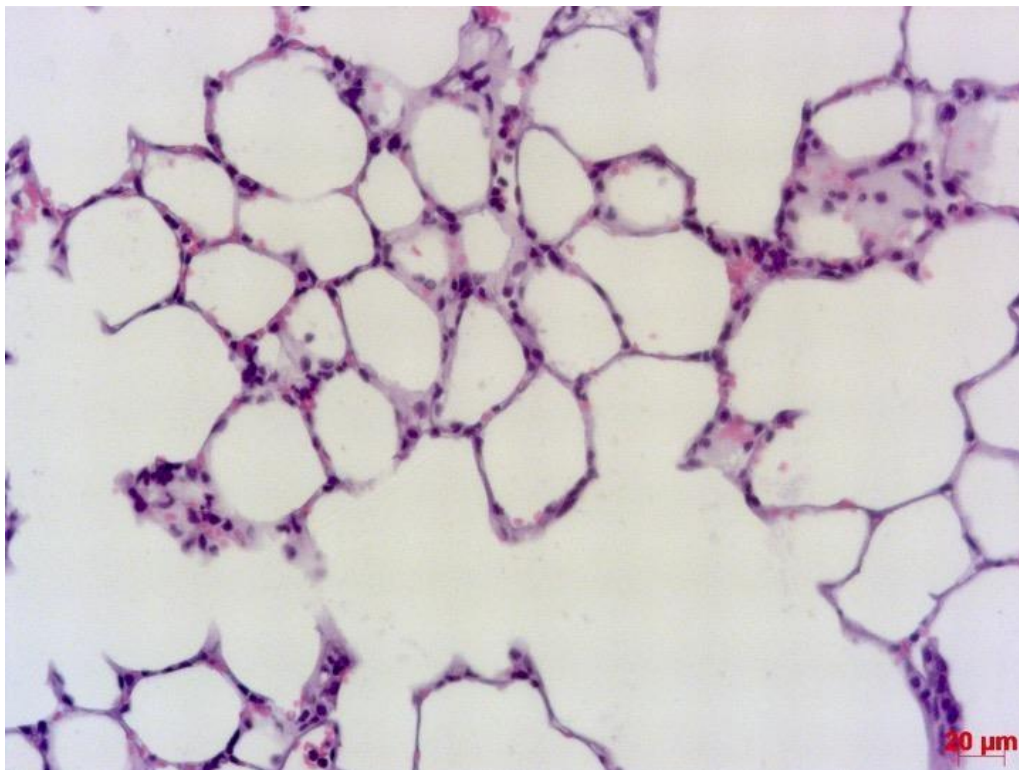


**Figure 22:** Exemplary histological specimen of a right lung, harvested after 90min of reperfusion (T2). Routine hematoxylin-eosin staining. Scale bar represents approximately 20 $\mu$ m.

The mean lung damage scores were  $0.73 \pm 0.03$  [aU] and  $0.61 \pm 0.08$  [aU] in left and right lung samples harvested at 90 min of reperfusion (T2), respectively. The difference was statistically significant (Figure 23;  $P=0.024$ ).

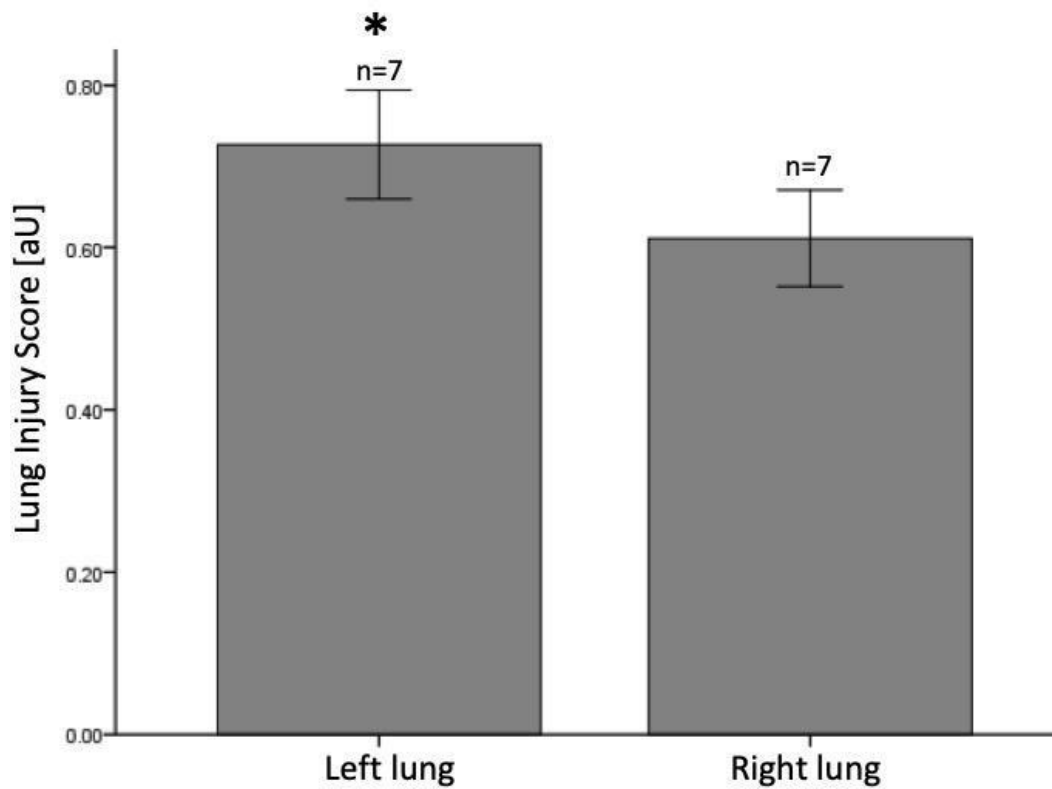


**Figure 23:** Lung injury Scores in left and right lung tissue specimens harvested after left-sided 30 min of ischemia and 90 min of reperfusion (T2). Data are given as mean values  $\pm$  standard error of the mean and n represents the number of experiments. The asterisk indicates a statistically significant difference ( $P<0.05$ ).

### *Histopathology of the heart*

The histopathologic analysis of cardiac tissue specimens harvested after 90 min of pulmonary reperfusion (at T2) showed a normal architecture of the myocardium (Figure 24), indicating no relevant effect of pulmonary ischemia/reperfusion injury on the myocardium at this time point.

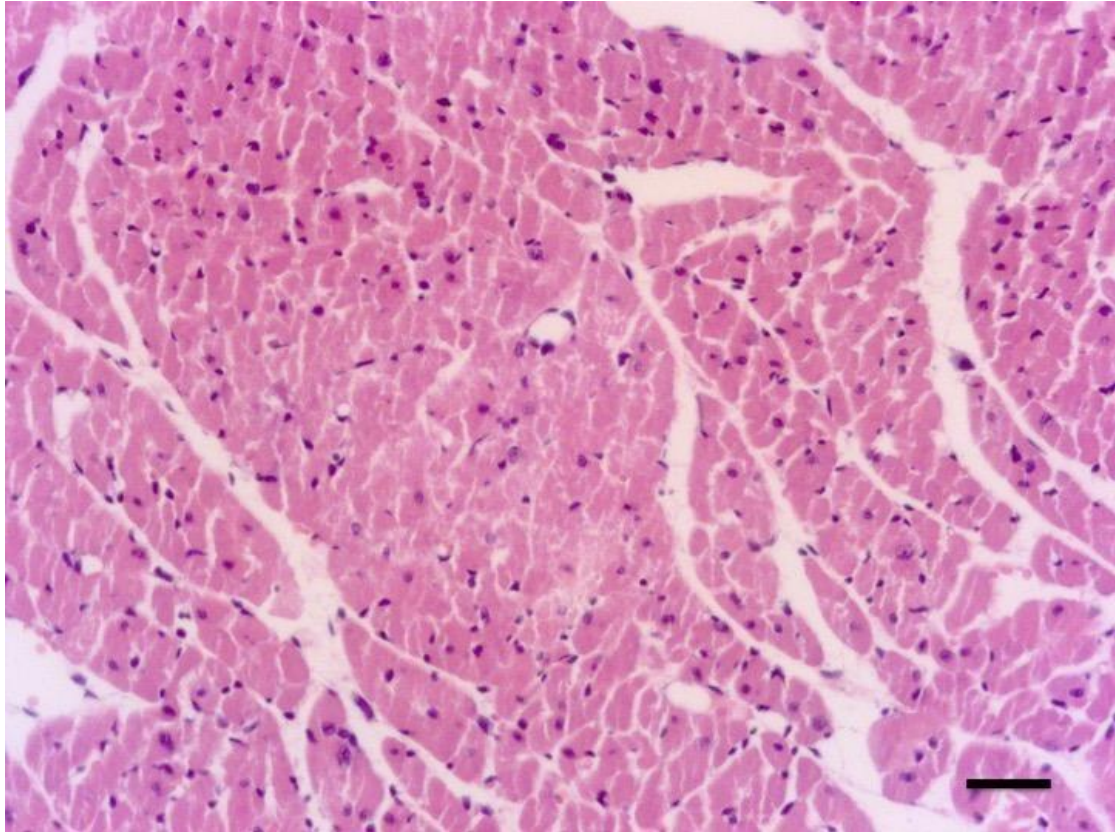


**Figure 24:** Histological specimen of the heart, harvested after 90min of pulmonary reperfusion (T2). Routine hematoxylin-eosin staining. Scale bar represents approximately 20µm.

### *Histopathology of the kidney*

The histopathologic analysis of kidney tissue specimens harvested after 90 min of pulmonary reperfusion (at T2) showed a vastly normal architecture (Figure 25), indicating no relevant effect of pulmonary ischemia/reperfusion injury on the kidney microarchitecture at this time point.

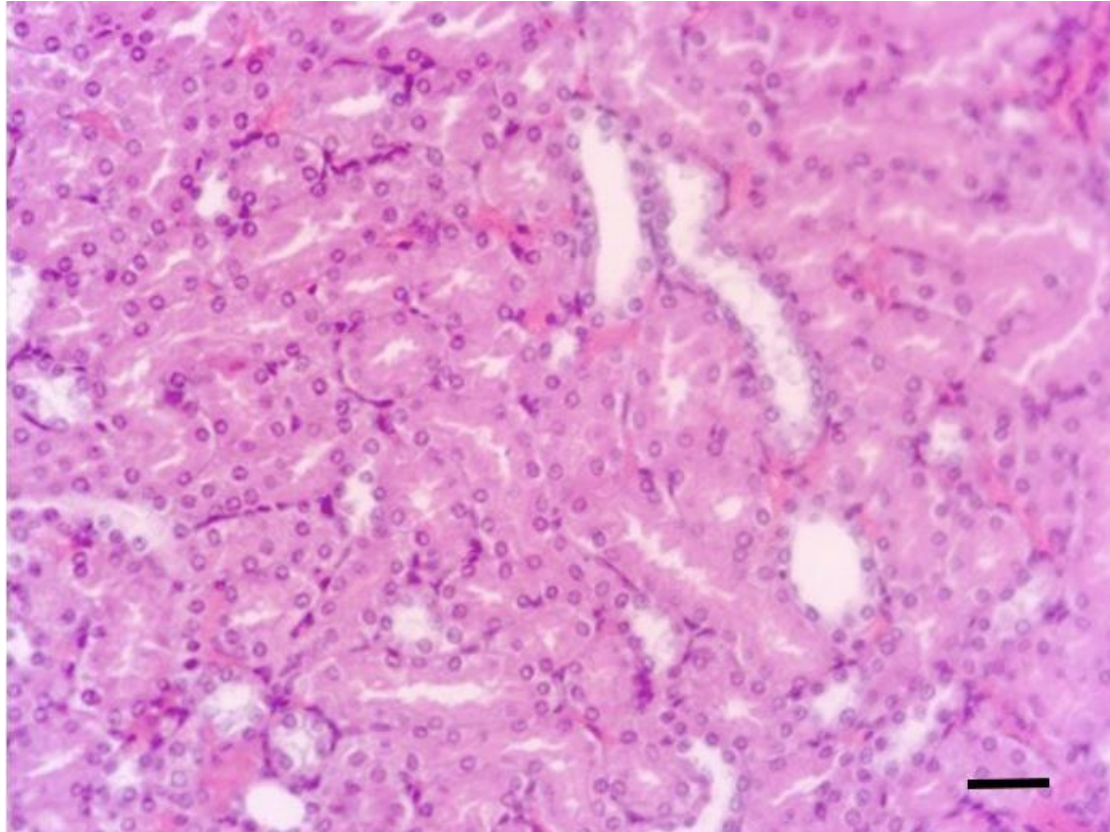


**Figure 25:** Histological specimen of a kidney harvested after 90min of pulmonary reperfusion (T2) showing relatively undisturbed tubular cellular architecture. Routine hematoxylin-eosin staining.

### *Histopathology of the liver*

The Suzuki Score [86] was used to semi-quantitatively quantify the secondary organ damage in the liver following pulmonary ischemia/reperfusion injury. Hepatocyte necrosis was not found in none of the liver specimens analysed. Instead, there were specimens with areas of hepatocyte congestion and vacuolization (Figure 26).

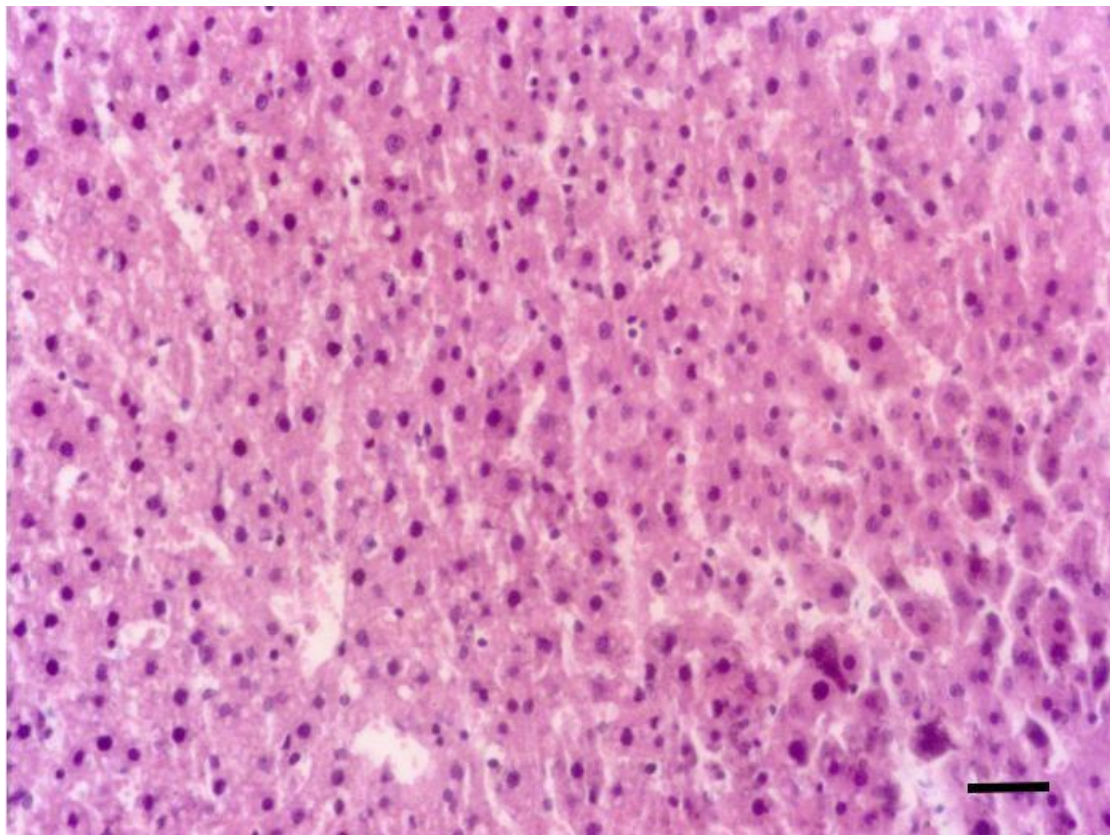


**Figure 26:** Histological specimen of a liver harvested after 90min of pulmonary reperfusion (T2) showing intense hepatocytic vacuolization. Routine hematoxylin-eosin staining. Scale bar represents approx. 20 micrometers.

Semi-quantitative analyses revealed a mean Suzuki Score for hepatocytic congestion and vacuolization of  $1.64 \pm 0.20$  [aU] and  $0.82 \pm 0.31$  [aU], respectively (Figure 27).

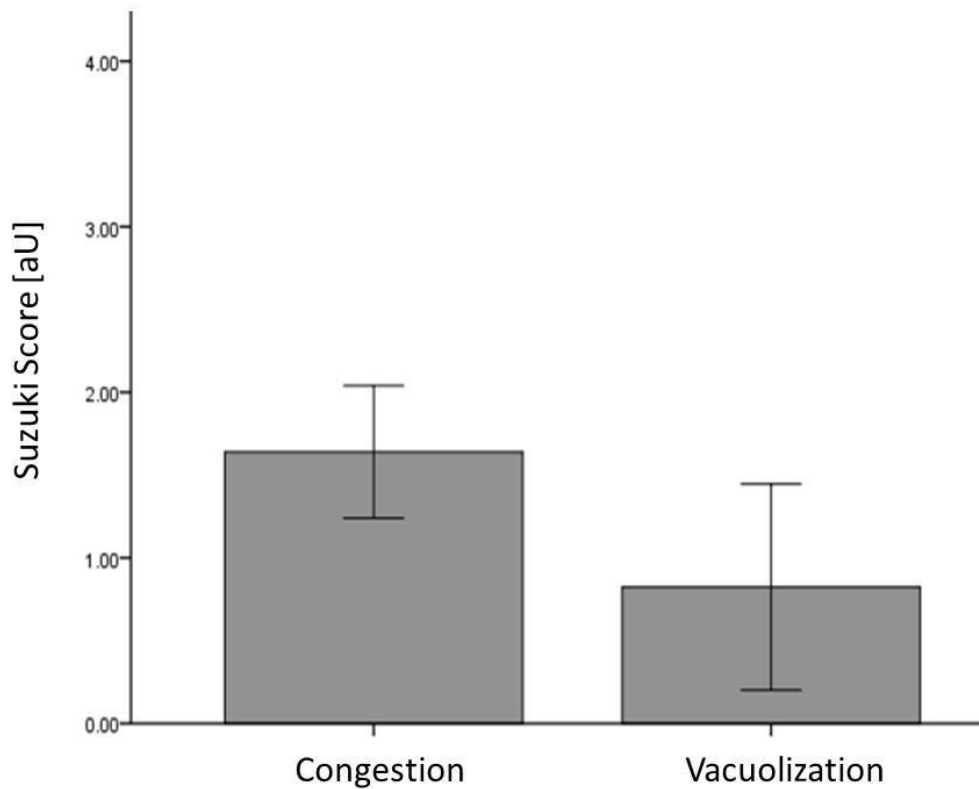


**Figure 27:** Secondary organ damage in the liver after pulmonary ischemia/reperfusion. Semi-quantitative histopathologic analysis was performed using the Suzuki-Score [ref], assessing hepatocytic congestion and vacuolization in liver specimens harvested at 90 min of pulmonary reperfusion (T2). Data are given as mean values  $\pm$  standard error of the mean (n=7).

## 7. Discussion

This study established an experimental approach to analyse cellular interactions and microcirculatory dysfunction during pulmonary ischemia/reperfusion injury by intravital fluorescence microscopy in the rat. While the experimentation of large experimental animals is appealing also in view of mimicking the human situation, it is challenging because of the demanding logistic efforts (housing, anaesthesia etc.). Small animal models are therefore preferred. Moreover, molecular targeting by genetic knock-out or knock-in techniques or pharmaco-immunological measures such as specific antibody treatment are well established and dramatically cheaper in rodents. Nevertheless, surgical preparation of the experimental animals and transplantation of solid organs for example in rodents is seemingly different from the larger experimental animal and human situations demanding meticulous microsurgical training and experience [87].

Experimental studies on pulmonary ischemia/reperfusion injury have been carried out in a large variety of animal models, e.g. in mice, rats, rabbits, dogs and sheep [36, 52, 70, 88, 89]. Some of these studies also investigated pulmonary ischemia/reperfusion injury and experimental lung transplantation. For example, early experimental works on lung transplantation analysed the effects of distinct lung graft inflation statuses during preservation [90-93]. Such insights in the relationship between graft inflation during procurement as well as transportation and post-transplant lung graft function have led to the generally accepted and practiced concept of clinical lung transplantation, harvesting and transporting lung allografts in a mild to moderately inflated state.

Many of the experimental studies on pulmonary ischemia/reperfusion injury intended to focus on microvascular dysfunction. A large variety of experiments indirectly assessed for example post-ischemic neutrophil accumulation in the lung by quantification of myeloperoxidase tissue content. Intravital fluorescence microscopy (IVM) has been extensively used and is a well established experimental and clinical means to observe and analyse microcirculatory phenomena under physiological and pathophysiological conditions in a large variety of organs [29, 77, 80, 94-96]. IVM of the thoracic organs is challenging because of the constant need for counterbalancing

the movements of the ventilated lung and the pulsations of the beating heart [97]. Kreisel and co-workers have used a veterinary glue to attach a cover glass onto the lung surface and found that neutrophil extravasation was monocyte-dependent in a challenging murine lung transplantation model [98]. However, the glue itself and/or the shear forces exerted by the moving lung after sticking to the glass slip may provoke distinct inflammatory responses affecting the pulmonary microcirculation apart from the desired pathophysiological setting of interest. Bennewitz et al. stabilized the lung surface by use of a specific suction system and analysed neutrophil and red blood cell trafficking in the pulmonary microcirculation in a model of sickle cell disease in mice [99]. Just as in the “glued lung”, there is some concern about potential extra shear force-induced “ventilator injury” in this approach [100]. Tabuchi et al. established a plateau phase at the end of the inspiration phase yielding a lung motion stop for 300ms before continuation with the respiratory cycle and thereby analysed the murine pulmonary microcirculation [101]. The herein used method also intended to establish an approach minimizing shear stress to the lung surface and excluding other toxic side effects potentially elicited by a glue. Access of the rat’s left lung subpleural pulmonary microcirculation for IVM was established as previously published in a murine model [102]. We used a cover glass slip that was fixed horizontally over the exposed lung surface by means of a micromanipulator. The level of the cover glass defined a stable focus level for the microscopic observations. The lung was attached to the lower side of the glass solely by hydrostatic forces after moistening its surface with warm physiological saline solution supported by a positive end-expiratory pressure level of 9mmHg [102]. Only horizontal excursions of the lung during inspiration and expiration were observed, but these did not hinder continuous visualization of the subpleural pulmonary microcirculation. Pulsations of the beating heart were found to be negligible choosing a target area in the lower lobe of the left lung. Supporting this technique, we had established this approach for IVM of the coronary microcirculation in rodents before [80, 103]

Despite all the technical advances, the use of IVM for studies on physiological and pathophysiological microcirculatory phenomena has some shortcomings. Obviously, there is a certain amount of surgical trauma that cannot be prevented for the exposure of the lung surface. It can only be minimized by refined microsurgical techniques. Direct manipulation of the target tissue must be omitted and the organs

surfaces must be kept moistened with temperature saline during the entire experimentation [104]. The experimental setup used herein is restricted for the acute experiment only. However, even though closure of the chest may be established, one has to consider that IVM of the lung surface at later time points after re-opening the chest may be hindered by ingrowth of adhesion tissues.

The use of fluorescent dyes such as FITC-dextrane or Rhodamine 6G may elicit a certain inflammatory and/or thrombogenic photo-toxic effect. This may be elicited by heat or induction of reactive oxygen species, both directly linked to the fluorescent light [105]. In fact, by extending the observation period, i.e. the tissue radiation with fluorescent light, Lindberg et al. could provoke platelet aggregation in the cremaster muscle preparation after injection of FITC dextrane [106]. Not only FITC dextrane, but also the use of Rhodamine 6G and extensive tissue exposure to fluorescent light may elicit platelet activation, endothelial cell damage, arteriolar vasospasm and leukocyte-endothelial cell interactions [107]. The photo-toxic effect may be used experimentally to study thrombogenesis in vivo [108]. Although it could not be eliminated, the photo-toxicity may not have relevantly affected the analyses in this present investigation, because the exposure of the lung surface to fluorescent light was kept to a minimum of only 20-30 seconds for the recording of the distinct regions of interest. Notably, visualization of clear-cut photo-toxic effects on the microcirculation may only be obtained after long exposure times and abnormally high light doses [109].

The experimental setup used in this investigation allows to visualize the pulmonary microcirculation of the rat in vivo under physiological conditions and after ischemia during reperfusion. The spatial and temporal resolution of the televised imaging enabled to analyse the circulation of blood through all segments of the rat's left lung subpleural pulmonary microcirculation. Using this approach, it is possible to clearly distinguish feeding pulmonary arterioles, alveolar capillaries and draining pulmonary post-capillary venules. We detected an inflammatory effect elicited by 30 minutes of pulmonary ischemia, i.e. IVM revealed an increase in leukocytic sequestration in the pulmonary microcirculation. In fact, there was a significant elevation of firmly attached leukocytes on the microvascular endothelium of post-capillary pulmonary venules as well as significantly increased numbers of sequestered leukocytes in pulmonary alveoli at 90 minutes of reperfusion. It needs to be noted that the lungs underwent 30 minutes of warm ischemia. Of course, this does not perfectly

mimic a lung transplantation model, but it offers to evaluate the true effect of ischemia on the pulmonary microcirculation, irrespective of any inflammatory reactions evoked by cooling and rewarming of a transplanted lung graft. The latter could be differentiated best by using a syngeneic transplantation approach, i.e. the transplantation of lungs between genetically identical individuals [110]. In addition, the herein presented approach allows to study pulmonary ischemia/reperfusion injury free of any cognate immune reactions as they cannot be excluded in an allogeneic transplantation model, i.e. the transplantation of a lung between genetically different individuals of the same species [111]. Importantly, using the rat model appeared advantageous over a murine approach perspective, because reproducibility of a murine lung transplantation is extremely difficult [112] and the rat may serve as a well established recipient when small animal xenotransplantation studies are intended, i.e. the transplantation of organs between individuals of different species. In fact, our group has recently published IVM studies of the coronary microcirculation in a hamster-to-rat heart transplantation model [82]. It has therefore been intriguing to establish an experimental basis for subsequent analyses of microvascular dysfunction in xenogeneic lung transplantation in a rodent model.

Microcirculatory dysfunction or a “no-reflow” phenomenon during reperfusion could not be delineated in the present study. Underlining this, there were no relevant alterations of microvascular diameters, neither in pulmonary terminal arterioles, alveolar capillaries nor post-capillary venules. Hence, a vasoreactive response following the ischemic period was not detected. In fact, the pulmonary microvascular blood flow remained relatively high. The timely resolution of the used image analyses software did not allow to determine blood flow velocities in the pulmonary microvessels, although this setup has been routinely used in other IVM settings [113, 114]. On one hand, the ischemic period may have been simply too short to elicit profound microcirculatory dysfunction during reperfusion. On the other hand, the observation period during reperfusion of the previously ischemic lung may have been too short to detect it. Sack and co-workers used a large animal lung transplantation model and found significant increases in pulmonary vascular resistance and reduced red blood cell flow velocities after 4 hours of cold ischemia and 6 hours of reperfusion [115]. IVM was used in a rabbit model of 1 hour of ischemia in the lung and the authors found reduced perfusion in alveolar capillaries and larger pulmonary microvessels after

10 min and 1 hour of reperfusion, respectively [62]. However, there was detectable microcirculatory dysfunction and inflammation during ischemia/reperfusion injury in the hamster-to-rat cardiac xenotransplantation model after comparable ischemic and reperfusion times as used in the present study[82]. The latter discrepancy very likely reflects the fact that the lung is more tolerant to ischemia than the heart or brain [116, 117]. As the lung is fed by arterial blood derived from the systemic circulation through bronchial arteries, one has to consider also that post-ischemic vasoreactivity may also occur in these vessels, which were inaccessible for epi-illumination IVM of the pleural lung surface. The lung is of entodermal origin and therefore it remains to be determined whether the bronchial arteries may have the potential to mimic the hepatic arterial buffer response [118].

Despite the lack of post-ischemic vasoreactions, there was a clearly detectable leukocytic response to the 30 minutes ischemic period during reperfusion. Significantly elevated numbers of Rhodamine 6G-stained leukocytes firmly attached to the pulmonary post-capillary venular endothelium and sequestered in the alveolar spaces at 90 minutes of reperfusion. Due to the polymorphonuclear staining characteristics of the interacting white blood cells, the present data underline previous findings suggesting that neutrophils play a significant role during pulmonary ischemia/reperfusion injury. Eppinger and colleagues analyzed the neutrophil sequestration in lung ischemia/reperfusion injury indirectly by measuring the pulmonary tissue content of myeloperoxidase [52]. They found significant neutrophil sequestration in reperfused rat lungs after 4 hours. Thus, the herein observed leukocytic response might have been even more pronounced in later reperfusion phases. Zhang et al., for example, quantified lung tissue neutrophil content by quantification of myeloperoxidase content 4 hours after Staphylococcal M1-protein induced pulmonary injury [119]. Interestingly, the data by Eppinger et al. suggest that there is a preceding inflammatory phase, independent of neutrophils and characterized by increased pulmonary vascular permeability early (30 minutes) during reperfusion [52]. They suggested that this early inflammation is driven by macrophages and the secretion of inflammatory mediators such as tumor necrosis factor (TNF)-alpha, interferon gamma and monocyte chemoattractant protein-1 [53]. Only TNF-alpha was involved in the neutrophil-dependent late inflammation phase and TNF-alpha is well known to provoke inflammatory neutrophil recruitment [77, 79, 120, 121]. It is interesting to note, that in

contrast to the findings by Eppinger et al., we found no evidence for an ischemia-induced increase in pulmonary microvascular permeability, despite the leukocytic response observed. Herein, macromolecular leakage and distances between alveolar spaces remained unaltered during reperfusion. The present findings, however, do not exclude the presence of macrophage-driven early post-ischemic permeability changes. The relative molecular weight of FITC-dextran is 150kDa and this dye may therefore be less effective in detecting mild pulmonary oedema formation, although it has been effectively used in other settings to quantify microvascular permeability [113, 122]. Again, the relatively small insult of only 30 minutes of ischemia may explain why vascular permeability changes might have been relatively small and were not detectable herein by IVM. The histopathological assessment and calculation of the lung damage score underline the latter notion. The detected lung tissue injury scores were found to be relatively low, although there was at least some degree of pulmonary edema detected from the histopathological analyses. However, there were virtually no hyaline membranes or proteinaceous debris within alveoli found, both of which are features in the clinical scenario of lung injury, but hardly found in animal models [123]. Looking at the semi-quantitative measures of the lung injury score, it seems less sensitive to detect mild pulmonary injury in animal models of lung injury [84].

Finding a leukocytic response to an ischemic insult in the reperfused lung microcirculation is *per se* not surprising as this is a general phenomenon observed in many other post-ischemic and reperfused organs [46-49]. Leukocyte influx is a feature of inflammation in general and neutrophils play a central role [124]. Also in the lung, neutrophil accumulation has been found in several inflammatory settings [102, 125, 126]. However, data on inflammatory leukocyte recruitment in the lung has to be interpreted carefully in view of the so-called “marginated pool” of leukocytes in the lung [127]. Even under normal and physiological conditions, there resides a large pool of leukocytes in the pulmonary tissue and this is different to other organs. It has been speculated that the passage of circulating leukocytes through alveolar capillaries is delayed because of the relatively small alveolar capillary diameters, therefore increasing the net lung tissue content of leukocytes under physiological conditions [63, 128, 129].

Although bronchial arteries are not accessible for IVM of the pleural surface of the lung, IVM is an effective mean to study the post-ischemic leukocyte infiltration into

the pulmonary tissue. Unaffected by the “marginated pool”, intravascular leukocyte-endothelial cell adhesive interactions can be visualized and quantified directly, as has also been reported previously [62, 102, 130, 131]. It cannot be excluded that circulating leukocytes may be recruited to the post-ischemic lung tissue by extravasation from bronchial arteries, but it is generally held that arterial vessels are not the prime location for inflammatory leukocyte recruitment [132, 133]. Only very small amounts of leukocytes may interact with arterial endothelium and that requires massive inflammatory stimulation when compared to venular endothelium. For example, after a local challenge with a relatively high-dosed cocktail of TNF-alpha and interleukin-1, mild leukocyte-endothelial cell adhesion occurred arteries, mediated by the integrin lymphocyte function-associated antigen (LFA)-1 [120]. In contrast to the relatively low response on the arterial endothelium, neighbouring venular endothelium was almost fully covered with adherent cells (unpublished data). The lesser leukocyte response in arteries may be explained by the fact that corresponding ligands for integrins, such as LFA-1, are only poorly expressed on arterial endothelium [133]. Even in atherosclerosis, it has been suggested that the vasa vasorum network (including venules) within the vessel wall of arteries are key players in the initiation and progression of this inflammatory vascular disease [134]. Circulating leukocytes may also be hindered to adhere to arterial endothelium because of the strikingly distinct shear rates in the arterial blood stream [133]. But it needs to be noted that blood flow in the low-pressure pulmonary arterial circulation differs tremendously from the systemic circulation. It was found herein that post-ischemic leukocyte-endothelial cell interactions take place primarily in postcapillary pulmonary venules, but not in pulmonary arterioles. This is in contrast to previous IVM studies on inflammatory leukocyte recruitment in the lung showing leukocyte endothelial cell adhesive interactions in both pulmonary arterioles and venules [102]. Others also observed rolling leukocytes in pulmonary microvessels, in both arterioles and venules [62, 125]. It can only be speculated at present whether the relatively small ischemic insult used herein may not allow to detect rolling interactions but only firm adhesion, which has to be considered to be a cumulative phenomenon in contrast to rolling.

Remote organ injury has been reported in several organs. For example, myocardial oedema formation and necrosis occur secondary to renal or hepatic ischemia/reperfusion injury [135]. Moderate acute kidney injury has been observed

during hepatic ischemia/reperfusion injury [136]. In turn, hepatic remote injury was observed after 30 minutes of intestinal ischemia and 90 minutes of reperfusion, presenting histopathologically with hepatocyte cytoplasmic clod formation, vacuolization and sinusoidal congestion [29]. Mechanistically, circulating inflammatory mediators derived from the primarily injured tissue and provided through a systemic inflammatory response elicit the injury in remote organs [137]. Herein, we found only mild hepatic affection after pulmonary ischemia and reperfusion, but no histopathological findings were obtained from cardiac and renal specimens. Potential reason is the only mild pulmonary ischemic insult, as discussed above. Nevertheless, despite the inflammatory response, remote organ injury during pulmonary ischemia and reperfusion may also be elicited hemodynamically. During lung transplantation, for example, clamping of one lung hilum leads to redirection of the entire cardiac output through only “half” of the pulmonary vascular bed. Although the pulmonary arteries are capacity vessels and may compensate volume overload through dilatation quite impressively under normal physiologic conditions, this function may be dramatically impaired in terminal lung diseases, which reason transplantation. In fact, end-stage lung disease patients frequently present with secondary pulmonary hypertension and therefore about 36% of lung transplantation procedures require the intraoperative use of extracorporeal circulation techniques in order to prevent acute right heart dilatation, congestion and ultimately failure [138].

Taken together, the presented experimental approach provides a basis for the experimental study of pulmonary ischemia/reperfusion injury by IVM in the rat. The experimental setup has been validated to study the entire subpleural pulmonary microcirculation before the induction of ischemia and during reperfusion. Future work on the microvascular dysfunction in the rat pulmonary ischemia/reperfusion injury model will have to focus more in detail on the ischemic time-reperfusion injury response relationship. However, IVM appears to be reliably used to study the pulmonary microcirculation in rats in experimental lung transplantation in the syngeneic, allogeneic and xenogeneic setting.

## 8. References

1. Meyer, K.C., *Recent advances in lung transplantation*. F1000Res, 2018. **7**.
2. Chambers, D.C., et al., *The International Thoracic Organ Transplant Registry of the International Society for Heart and Lung Transplantation: Thirty-sixth adult lung and heart-lung transplantation Report-2019; Focus theme: Donor and recipient size match*. J Heart Lung Transplant, 2019. **38**(10): p. 1042-1055.
3. Kiziltug, H. and F. Falter, *Circulatory support during lung transplantation*. Curr Opin Anaesthesiol, 2020. **33**(1): p. 37-42.
4. Chung, P.A. and D.F. Dilling, *Immunosuppressive strategies in lung transplantation*. Ann Transl Med, 2020. **8**(6): p. 409.
5. Chambers, D.C., et al., *The Registry of the International Society for Heart and Lung Transplantation: Thirty-fourth Adult Lung And Heart-Lung Transplantation Report-2017; Focus Theme: Allograft ischemic time*. J Heart Lung Transplant, 2017. **36**(10): p. 1047-1059.
6. Eltzschig, H.K. and T. Eckle, *Ischemia and reperfusion--from mechanism to translation*. Nat Med, 2011. **17**(11): p. 1391-401.
7. Ius, F., et al., *Preemptive treatment of early donor-specific antibodies with IgA- and IgM-enriched intravenous human immunoglobulins in lung transplantation*. Am J Transplant, 2018. **18**(9): p. 2295-2304.
8. Verleden, G.M., et al., *Chronic lung allograft dysfunction: Definition, diagnostic criteria, and approaches to treatment-A consensus report from the Pulmonary Council of the ISHLT*. J Heart Lung Transplant, 2019. **38**(5): p. 493-503.
9. Gielis, J.F., et al., *Oxidative and nitrosative stress during pulmonary ischemia-reperfusion injury: from the lab to the OR*. Ann Transl Med, 2017. **5**(6): p. 131.
10. Weyker, P.D., et al., *Lung ischemia reperfusion injury: a bench-to-bedside review*. Semin Cardiothorac Vasc Anesth, 2013. **17**(1): p. 28-43.
11. Fischer, S., et al., *Low-potassium dextran preservation solution improves lung function after human lung transplantation*. J Thorac Cardiovasc Surg, 2001. **121**(3): p. 594-6.

12. Struber, M., et al., *Flush perfusion with low potassium dextran solution improves early graft function in clinical lung transplantation*. Eur J Cardiothorac Surg, 2001. **19**(2): p. 190-4.
13. Grimm, J.C., et al., *Association Between Prolonged Graft Ischemia and Primary Graft Failure or Survival Following Lung Transplantation*. JAMA Surg, 2015. **150**(6): p. 547-53.
14. Hayes, D., Jr., et al., *Influence of graft ischemic time and geographic distance between donor and recipient on survival in children after lung transplantation*. J Heart Lung Transplant, 2016. **35**(10): p. 1220-1226.
15. Shigemura, N., S. Tane, and K. Noda, *The Bronchial Arterial Circulation in Lung Transplantation: Bedside to Bench to Bedside, and Beyond*. Transplantation, 2018. **102**(8): p. 1240-1249.
16. Siegelman, S.S., et al., *Restoration of bronchial artery circulation after canine lung allotransplantation*. J Thorac Cardiovasc Surg, 1977. **73**(5): p. 792-5.
17. Shah, R.J. and J.M. Diamond, *Primary Graft Dysfunction (PGD) Following Lung Transplantation*. Semin Respir Crit Care Med, 2018. **39**(2): p. 148-154.
18. Diamond, J.M., et al., *Clinical risk factors for primary graft dysfunction after lung transplantation*. Am J Respir Crit Care Med, 2013. **187**(5): p. 527-34.
19. Yusef, R.D., et al., *The Registry of the International Society for Heart and Lung Transplantation: Thirty-third Adult Lung and Heart-Lung Transplant Report-2016; Focus Theme: Primary Diagnostic Indications for Transplant*. J Heart Lung Transplant, 2016. **35**(10): p. 1170-1184.
20. Snell, G.I., et al., *Report of the ISHLT Working Group on Primary Lung Graft Dysfunction, part I: Definition and grading-A 2016 Consensus Group statement of the International Society for Heart and Lung Transplantation*. J Heart Lung Transplant, 2017. **36**(10): p. 1097-1103.
21. Loo, G., et al., *Portable normothermic ex-vivo lung perfusion, ventilation, and functional assessment with the Organ Care System on donor lung use for transplantation from extended-criteria donors (EXPAND): a single-arm, pivotal trial*. Lancet Respir Med, 2019. **7**(11): p. 975-984.
22. Warnecke, G., et al., *Normothermic ex-vivo preservation with the portable Organ Care System Lung device for bilateral lung transplantation (INSPIRE): a randomised, open-label, non-inferiority, phase 3 study*. Lancet Respir Med, 2018. **6**(5): p. 357-367.

23. Hotchkiss, R.S., et al., *Cell death*. N Engl J Med, 2009. **361**(16): p. 1570-83.
24. Al-Mehdi, A.B., et al., *Endothelial NADPH oxidase as the source of oxidants in lungs exposed to ischemia or high K<sup>+</sup>*. Circ Res, 1998. **83**(7): p. 730-7.
25. Kennedy, T.P., et al., *Role of reactive oxygen species in reperfusion injury of the rabbit lung*. J Clin Invest, 1989. **83**(4): p. 1326-35.
26. Pak, O., et al., *Lung Ischaemia-Reperfusion Injury: The Role of Reactive Oxygen Species*. Adv Exp Med Biol, 2017. **967**: p. 195-225.
27. Kloner, R.A., et al., *Ultrastructural evidence of microvascular damage and myocardial cell injury after coronary artery occlusion: which comes first?* Circulation, 1980. **62**(5): p. 945-52.
28. Kloner, R.A., K.S. King, and M.G. Harrington, *No-reflow phenomenon in the heart and brain*. Am J Physiol Heart Circ Physiol, 2018. **315**(3): p. H550-h562.
29. Schramm, R., et al., *Atherosclerosis aggravates ischemia/reperfusion injury in the gut and remote damage in the liver and the lung*. Inflamm Res, 2011. **60**(6): p. 555-67.
30. Schramm, R., *Tracking leukocyte adhesion molecule function in lymphocyte homing and transplant rejection*. 2008. p. 91 Bl.
31. Land, W.G., *Emerging role of innate immunity in organ transplantation: part I: evolution of innate immunity and oxidative allograft injury*. Transplant Rev (Orlando), 2012. **26**(2): p. 60-72.
32. Fairchild, R.L. and J.S. Bromberg, *Molecular assassins from within: intracellular DAMPs from injured cells initiate tissue inflammation*. Am J Transplant, 2012. **12**(12): p. 3169.
33. Chen, G.Y. and G. Nunez, *Sterile inflammation: sensing and reacting to damage*. Nat Rev Immunol, 2010. **10**(12): p. 826-37.
34. Soehnlein, O. and L. Lindbom, *Phagocyte partnership during the onset and resolution of inflammation*. Nat Rev Immunol, 2010. **10**(6): p. 427-39.
35. Naidu, B.V., et al., *Early activation of the alveolar macrophage is critical to the development of lung ischemia-reperfusion injury*. J Thorac Cardiovasc Surg, 2003. **126**(1): p. 200-7.
36. Prakash, A., et al., *Alveolar macrophages and Toll-like receptor 4 mediate ventilated lung ischemia reperfusion injury in mice*. Anesthesiology, 2012. **117**(4): p. 822-35.

37. Madjdpour, C., et al., *Decreased alveolar oxygen induces lung inflammation*. Am J Physiol Lung Cell Mol Physiol, 2003. **284**(2): p. L360-7.
38. Tsushima, Y., et al., *The depletion of donor macrophages reduces ischaemia-reperfusion injury after mouse lung transplantation*. Eur J Cardiothorac Surg, 2014. **45**(4): p. 703-9.
39. Merry, H.E., et al., *Role of toll-like receptor-4 in lung ischemia-reperfusion injury*. Ann Thorac Surg, 2015. **99**(4): p. 1193-9.
40. Rancan, L., et al., *Chemokine Involvement in Lung Injury Secondary to Ischaemia/Reperfusion*. Lung, 2017. **195**(3): p. 333-340.
41. Zhao, M., et al., *Alveolar macrophage activation is a key initiation signal for acute lung ischemia-reperfusion injury*. Am J Physiol Lung Cell Mol Physiol, 2006. **291**(5): p. L1018-26.
42. Zhu, B., et al., *The attenuation of lung ischemia reperfusion injury by oxymatrine*. Cell Biochem Biophys, 2014. **70**(1): p. 333-6.
43. Chiu, S. and A. Bharat, *Role of monocytes and macrophages in regulating immune response following lung transplantation*. Curr Opin Organ Transplant, 2016. **21**(3): p. 239-45.
44. Hsiao, H.M., et al., *Spleen-derived classical monocytes mediate lung ischemia-reperfusion injury through IL-1beta*. J Clin Invest, 2018.
45. Zheng, Z., et al., *Donor pulmonary intravascular nonclassical monocytes recruit recipient neutrophils and mediate primary lung allograft dysfunction*. Sci Transl Med, 2017. **9**(394).
46. Oliveira, T.H.C., et al., *Neutrophils: a cornerstone of liver ischemia and reperfusion injury*. Lab Invest, 2018. **98**(1): p. 51-62.
47. Hashimoto, S., et al., *Intravital imaging of neutrophil recruitment in intestinal ischemia-reperfusion injury*. Biochem Biophys Res Commun, 2018. **495**(3): p. 2296-2302.
48. Kezic, A., N. Stajic, and F. Thaiss, *Innate Immune Response in Kidney Ischemia/Reperfusion Injury: Potential Target for Therapy*. J Immunol Res, 2017. **2017**: p. 6305439.
49. Li, W., et al., *Ferroptotic cell death and TLR4/Trif signaling initiate neutrophil recruitment after heart transplantation*. J Clin Invest, 2019. **129**(6): p. 2293-2304.

50. Deeb, G.M., et al., *Neutrophils are not necessary for induction of ischemia-reperfusion lung injury*. J Appl Physiol (1985), 1990. **68**(1): p. 374-81.
51. Steimle, C.N., et al., *Neutrophils are not necessary for ischemia-reperfusion lung injury*. Ann Thorac Surg, 1992. **53**(1): p. 64-72; discussion 72-3.
52. Eppinger, M.J., et al., *Pattern of injury and the role of neutrophils in reperfusion injury of rat lung*. J Surg Res, 1995. **58**(6): p. 713-8.
53. Eppinger, M.J., et al., *Mediators of ischemia-reperfusion injury of rat lung*. Am J Pathol, 1997. **150**(5): p. 1773-84.
54. Morrison, M.I., T.L. Pither, and A.J. Fisher, *Pathophysiology and classification of primary graft dysfunction after lung transplantation*. J Thorac Dis, 2017. **9**(10): p. 4084-4097.
55. Williams, A.E. and R.C. Chambers, *The mercurial nature of neutrophils: still an enigma in ARDS?* Am J Physiol Lung Cell Mol Physiol, 2014. **306**(3): p. L217-30.
56. Hamacher, J., et al., *Ebselen improves ischemia-reperfusion injury after rat lung transplantation*. Lung, 2009. **187**(2): p. 98-103.
57. Harada, M., et al., *A neutrophil elastase inhibitor improves lung function during ex vivo lung perfusion*. Gen Thorac Cardiovasc Surg, 2015. **63**(12): p. 645-51.
58. Brinkmann, V., et al., *Neutrophil extracellular traps kill bacteria*. Science, 2004. **303**(5663): p. 1532-5.
59. Caudrillier, A., et al., *Platelets induce neutrophil extracellular traps in transfusion-related acute lung injury*. J Clin Invest, 2012. **122**(7): p. 2661-71.
60. Sayah, D.M., et al., *Neutrophil extracellular traps are pathogenic in primary graft dysfunction after lung transplantation*. Am J Respir Crit Care Med, 2015. **191**(4): p. 455-63.
61. Lien, D.C., et al., *Neutrophil kinetics in the pulmonary microcirculation. Effects of pressure and flow in the dependent lung*. Am Rev Respir Dis, 1990. **141**(4 Pt 1): p. 953-9.
62. Kuhnle, G.E., F.H. Leipfinger, and A.E. Goetz, *Measurement of microhemodynamics in the ventilated rabbit lung by intravital fluorescence microscopy*. J Appl Physiol (1985), 1993. **74**(3): p. 1462-71.

63. Kuebler, W.M., et al., *Leukocyte kinetics in pulmonary microcirculation: intravital fluorescence microscopic study*. J Appl Physiol (1985), 1994. **76**(1): p. 65-71.
64. Daniel, J.L., et al., *Molecular basis for ADP-induced platelet activation. I. Evidence for three distinct ADP receptors on human platelets*. J Biol Chem, 1998. **273**(4): p. 2024-9.
65. Brass, L.F., *Thrombin and platelet activation*. Chest, 2003. **124**(3 Suppl): p. 18s-25s.
66. Canobbio, I., et al., *Platelet activation by von Willebrand factor requires coordinated signaling through thromboxane A2 and Fc gamma IIA receptor*. J Biol Chem, 2001. **276**(28): p. 26022-9.
67. Massberg, S., et al., *Platelet-endothelial cell interactions during ischemia/reperfusion: the role of P-selectin*. Blood, 1998. **92**(2): p. 507-15.
68. Dixon, J.T., E. Gozal, and A.M. Roberts, *Platelet-mediated vascular dysfunction during acute lung injury*. Arch Physiol Biochem, 2012. **118**(2): p. 72-82.
69. Eltzschig, H.K. and C.D. Collard, *Vascular ischaemia and reperfusion injury*. Br Med Bull, 2004. **70**: p. 71-86.
70. Klausner, J.M., et al., *Reperfusion pulmonary edema*. Jama, 1989. **261**(7): p. 1030-5.
71. Diamond, J.M., et al., *Elevated plasma angiopoietin-2 levels and primary graft dysfunction after lung transplantation*. PLoS One, 2012. **7**(12): p. e51932.
72. Abraham, D., et al., *VEGF-A and -C but not -B mediate increased vascular permeability in preserved lung grafts*. Transplantation, 2002. **73**(11): p. 1703-6.
73. Chen, K.H., et al., *Ischemia and reperfusion of the lung tissues induced increase of lung permeability and lung edema is attenuated by dimethylthiourea (PP69)*. Transplant Proc, 2010. **42**(3): p. 748-50.
74. Zhao, X., et al., *Hypoxia-inducible factor 1 alpha contributes to pulmonary vascular dysfunction in lung ischemia-reperfusion injury*. Int J Clin Exp Pathol, 2014. **7**(6): p. 3081-8.

75. Stone, M.L., et al., *Sphingosine-1-phosphate receptor 1 agonism attenuates lung ischemia-reperfusion injury*. *Am J Physiol Lung Cell Mol Physiol*, 2015. **308**(12): p. L1245-52.
76. Mallavia, B., et al., *Inhibiting Integrin alphavbeta5 Reduces Ischemia-Reperfusion Injury in an Orthotopic Lung Transplant Model in Mice*. *Am J Transplant*, 2016. **16**(4): p. 1306-11.
77. Klintman, D., et al., *Leukocyte recruitment in hepatic injury: selectin-mediated leukocyte rolling is a prerequisite for CD18-dependent firm adhesion*. *J Hepatol*, 2002. **36**(1): p. 53-9.
78. Riaz, A.A., et al., *Fundamental and distinct roles of P-selectin and LFA-1 in ischemia/reperfusion-induced leukocyte-endothelium interactions in the mouse colon*. *Ann Surg*, 2002. **236**(6): p. 777-84; discussion 784.
79. Wan, M.X., et al., *CC chemokines induce P-selectin-dependent neutrophil rolling and recruitment in vivo: intermediary role of mast cells*. *Br J Pharmacol*, 2003. **138**(4): p. 698-706.
80. Schramm, R., et al., *The subepicardial microcirculation in heterotopically transplanted mouse hearts: an intravital multicolor fluorescence microscopy study*. *J Thorac Cardiovasc Surg*, 2007. **134**(1): p. 210-7, 217 e1.
81. Roller, J., et al., *How to detect a dwarf: in vivo imaging of nanoparticles in the lung*. *Nanomedicine*, 2011. **7**(6): p. 753-62.
82. Geiger, D., et al., *The Coronary Microcirculation in Hamster-to-Rat Cardiac Xenografts*. *Eur Surg Res*, 2015. **55**(4): p. 364-373.
83. Gielis, J.F., et al., *A murine model of lung ischemia and reperfusion injury: tricks of the trade*. *J Surg Res*, 2015. **194**(2): p. 659-66.
84. Matute-Bello, G., et al., *An official American Thoracic Society workshop report: features and measurements of experimental acute lung injury in animals*. *Am J Respir Cell Mol Biol*, 2011. **44**(5): p. 725-38.
85. Yamauchi, J., et al., *Improvement of microvascular graft equilibration and preservation in non-heart-beating donors by warm preflush with streptokinase*. *Transplantation*, 2003. **75**(4): p. 449-53.
86. Suzuki, S., et al., *Neutrophil infiltration as an important factor in liver ischemia and reperfusion injury. Modulating effects of FK506 and cyclosporine*. *Transplantation*, 1993. **55**(6): p. 1265-72.

87. Bribriescio, A.C., et al., *Experimental models of lung transplantation*. Front Biosci (Elite Ed), 2013. **5**: p. 266-72.
88. Roberts, A.M., et al., *Effects of pulmonary ischemia-reperfusion on platelet adhesion in subpleural arterioles in rabbits*. Microvasc Res, 2004. **67**(1): p. 29-37.
89. Bishop, M.J., et al., *Reperfusion of ischemic dog lung results in fever, leukopenia, and lung edema*. Am Rev Respir Dis, 1986. **134**(4): p. 752-6.
90. Veith, F.J., et al., *Effective preservation and transportation of lung transplants*. J Thorac Cardiovasc Surg, 1976. **72**(1): p. 97-105.
91. Stevens, G.H., M.M. Sanchez, and G.L. Chappell, *Enhancement of lung preservation by prevention of lung collapse*. J Surg Res, 1973. **14**(5): p. 400-5.
92. Puskas, J.D., et al., *Reliable thirty-hour lung preservation by donor lung hyperinflation*. J Thorac Cardiovasc Surg, 1992. **104**(4): p. 1075-83.
93. Dreyfuss, D. and G. Saumon, *Ventilator-induced lung injury: lessons from experimental studies*. Am J Respir Crit Care Med, 1998. **157**(1): p. 294-323.
94. Schramm, R., et al., *Statins inhibit lymphocyte homing to peripheral lymph nodes*. Immunology, 2007. **120**(3): p. 315-24.
95. Schramm, R., et al., *Blockade of in vivo VEGF-KDR/flk-1 signaling does not affect revascularization of freely transplanted pancreatic islets*. Transplantation, 2003. **75**(2): p. 239-42.
96. De Niz, M., A. Nacer, and F. Frischknecht, *Intravital microscopy: Imaging host-parasite interactions in the brain*. Cell Microbiol, 2019. **21**(5): p. e13024.
97. Fiole, D. and J.N. Tournier, *Intravital microscopy of the lung: minimizing invasiveness*. J Biophotonics, 2016. **9**(9): p. 868-78.
98. Kreisel, D., et al., *In vivo two-photon imaging reveals monocyte-dependent neutrophil extravasation during pulmonary inflammation*. Proc Natl Acad Sci U S A, 2010. **107**(42): p. 18073-8.
99. Bennewitz, M.F., S.C. Watkins, and P. Sundd, *Quantitative intravital two-photon excitation microscopy reveals absence of pulmonary vaso-occlusion in unchallenged Sickle Cell Disease mice*. Intravital, 2014. **3**(2): p. e29748.
100. Yang, Y., G. Yang, and E.P. Schmidt, *In vivo measurement of the mouse pulmonary endothelial surface layer*. J Vis Exp, 2013(72): p. e50322.
101. Tabuchi, A., et al., *Intravital microscopy of the murine pulmonary microcirculation*. J Appl Physiol (1985), 2008. **104**(2): p. 338-46.

102. Roller, J., et al., *Direct in vivo observations of P-selectin glycoprotein ligand-1-mediated leukocyte-endothelial cell interactions in the pulmonary microvasculature in abdominal sepsis in mice*. *Inflamm Res*, 2013. **62**(3): p. 275-82.
103. Schramm, R., et al., *Erythropoietin inhibits post-ischemic leukocyte adhesion but does not affect rejection in murine cardiac allografts*. *J Heart Lung Transplant*, 2010. **29**(10): p. 1185-92.
104. Tschernig, T., et al., *Direct visualisation of microparticles in the living lung*. *Exp Toxicol Pathol*, 2013. **65**(6): p. 883-6.
105. Povlishock, J.T., et al., *An ultrastructural analysis of endothelial change paralleling platelet aggregation in a light/dye model of microvascular insult*. *Am J Pathol*, 1983. **110**(2): p. 148-60.
106. Lindberg, R.A., et al., *Involvement of nitric oxide and cyclooxygenase products in photoactivation-induced microvascular occlusion*. *Microvasc Res*, 1994. **47**(2): p. 203-21.
107. Saetzler, R.K., et al., *Intravital fluorescence microscopy: impact of light-induced phototoxicity on adhesion of fluorescently labeled leukocytes*. *J Histochem Cytochem*, 1997. **45**(4): p. 505-13.
108. Grambow, E., et al., *Differential effects of endogenous, phyto and synthetic cannabinoids on thrombogenesis and platelet activity*. *Biofactors*, 2016. **42**(6): p. 581-590.
109. Steinbauer, M., et al., *Characterization and prevention of phototoxic effects in intravital fluorescence microscopy in the hamster dorsal skinfold model*. *Langenbecks Arch Surg*, 2000. **385**(4): p. 290-8.
110. Schueler, S., et al., *Successful twenty-four-hour lung preservation with donor core cooling and leukocyte depletion in an orthotopic double lung transplantation model*. *J Thorac Cardiovasc Surg*, 1992. **104**(1): p. 73-82.
111. Lafferty, K.J. and J. Woolnough, *The origin and mechanism of the allograft reaction*. *Immunol Rev*, 1977. **35**: p. 231-62.
112. Jungraithmayr, W.M., et al., *A mouse model of orthotopic, single-lung transplantation*. *J Thorac Cardiovasc Surg*, 2009. **137**(2): p. 486-91.
113. Reichel, C.A., et al., *Gelatinases mediate neutrophil recruitment in vivo: evidence for stimulus specificity and a critical role in collagen IV remodeling*. *J Leukoc Biol*, 2008. **83**(4): p. 864-74.

114. Mempel, T.R., et al., *Visualization of leukocyte transendothelial and interstitial migration using reflected light oblique transillumination in intravital video microscopy*. *J Vasc Res*, 2003. **40**(5): p. 435-41.
115. Sack, F.U., et al., *Intravital microscopy of pulmonary microcirculation after single lung transplantation in pigs*. *Transplant Proc*, 2006. **38**(3): p. 737-40.
116. Ames, A., 3rd, et al., *Cerebral ischemia. II. The no-reflow phenomenon*. *Am J Pathol*, 1968. **52**(2): p. 437-53.
117. Kolwicz, S.C., Jr., S. Purohit, and R. Tian, *Cardiac metabolism and its interactions with contraction, growth, and survival of cardiomyocytes*. *Circ Res*, 2013. **113**(5): p. 603-16.
118. Richter, S., et al., *Hepatic arteriolo-portal venular shunting guarantees maintenance of nutritional microvascular supply in hepatic arterial buffer response of rat livers*. *J Physiol*, 2001. **531**(Pt 1): p. 193-201.
119. Zhang, S., et al., *Streptococcal M1 protein-induced lung injury is independent of platelets in mice*. *Shock*, 2011. **35**(1): p. 86-91.
120. Schramm, R., et al., *Leukocyte adhesion in aorta and femoral artery in vivo is mediated by LFA-1*. *Inflamm Res*, 2004. **53**(10): p. 523-7.
121. Zhang, X.W., et al., *Important role of CD18 in TNF-alpha-induced leukocyte adhesion in muscle and skin venules in vivo*. *Inflamm Res*, 2000. **49**(10): p. 529-34.
122. Reichel, C.A., et al., *Urokinase-type plasminogen activator promotes paracellular transmigration of neutrophils via Mac-1, but independently of urokinase-type plasminogen activator receptor*. *Circulation*, 2011. **124**(17): p. 1848-59.
123. Aeffner, F., B. Bolon, and I.C. Davis, *Mouse Models of Acute Respiratory Distress Syndrome: A Review of Analytical Approaches, Pathologic Features, and Common Measurements*. *Toxicol Pathol*, 2015. **43**(8): p. 1074-92.
124. Pham, C.T., *Neutrophil serine proteases: specific regulators of inflammation*. *Nat Rev Immunol*, 2006. **6**(7): p. 541-50.
125. Wang, Y., et al., *Distinct patterns of leukocyte recruitment in the pulmonary microvasculature in response to local and systemic inflammation*. *Am J Physiol Lung Cell Mol Physiol*, 2013. **304**(4): p. L298-305.

126. Rahman, M., et al., *Metalloproteinases regulate CD40L shedding from platelets and pulmonary recruitment of neutrophils in abdominal sepsis*. *Inflamm Res*, 2012. **61**(6): p. 571-9.
127. Kuebler, W.M. and A.E. Goetz, *The marginated pool*. *Eur Surg Res*, 2002. **34**(1-2): p. 92-100.
128. Kuebler, W.M., G.E. Kuhnle, and A.E. Goetz, *Leukocyte margination in alveolar capillaries: interrelationship with functional capillary geometry and microhemodynamics*. *J Vasc Res*, 1999. **36**(4): p. 282-8.
129. Kuhnle, G.E., et al., *Effect of blood flow on the leukocyte-endothelium interaction in pulmonary microvessels*. *Am J Respir Crit Care Med*, 1995. **152**(4 Pt 1): p. 1221-8.
130. Kuebler, W.M., et al., *Role of L-selectin in leukocyte sequestration in lung capillaries in a rabbit model of endotoxemia*. *Am J Respir Crit Care Med*, 2000. **161**(1): p. 36-43.
131. Kuebler, W.M., et al., *Contribution of selectins to leukocyte sequestration in pulmonary microvessels by intravital microscopy in rabbits*. *J Physiol*, 1997. **501** ( Pt 2)(Pt 2): p. 375-86.
132. Atherton, A. and G.V. Born, *Relationship between the velocity of rolling granulocytes and that of the blood flow in venules*. *J Physiol*, 1973. **233**(1): p. 157-65.
133. Perry, M.A. and D.N. Granger, *Role of CD11/CD18 in shear rate-dependent leukocyte-endothelial cell interactions in cat mesenteric venules*. *J Clin Invest*, 1991. **87**(5): p. 1798-804.
134. Sedding, D.G., et al., *Vasa Vasorum Angiogenesis: Key Player in the Initiation and Progression of Atherosclerosis and Potential Target for the Treatment of Cardiovascular Disease*. *Front Immunol*, 2018. **9**: p. 706.
135. Youssef, M.I., A.A. Mahmoud, and R.H. Abdelghany, *A new combination of sitagliptin and furosemide protects against remote myocardial injury induced by renal ischemia/reperfusion in rats*. *Biochem Pharmacol*, 2015. **96**(1): p. 20-9.
136. Lee, H.T., et al., *Acute kidney injury after hepatic ischemia and reperfusion injury in mice*. *Lab Invest*, 2009. **89**(2): p. 196-208.
137. Nastos, C., et al., *Global consequences of liver ischemia/reperfusion injury*. *Oxid Med Cell Longev*, 2014. **2014**: p. 906965.

138. Hinske, L.C., et al., *Predicting the Necessity for Extracorporeal Circulation During Lung Transplantation: A Feasibility Study*. J Cardiothorac Vasc Anesth, 2017. **31**(3): p. 931-938.



LUDWIG-  
MAXIMILIANS-  
UNIVERSITÄT  
MÜNCHEN

Promotionsbüro  
Medizinische Fakultät



## Eidesstattliche Versicherung

Na, Rongrui

Name, Vorname

Ich erkläre hiermit an Eides statt,

dass ich die vorliegende Dissertation mit dem Titel

Intravital microscopy of lung ischemia reperfusion injury in a rat model

selbständig verfasst, mich außer der angegebenen keiner weiteren Hilfsmittel bedient und alle Erkenntnisse, die aus dem Schrifttum ganz oder annähernd übernommen sind, als solche kenntlich gemacht und nach ihrer Herkunft unter Bezeichnung der Fundstelle einzeln nachgewiesen habe.

Ich erkläre des Weiteren, dass die hier vorgelegte Dissertation nicht in gleicher oder in ähnlicher Form bei einer anderen Stelle zur Erlangung eines akademischen Grades eingereicht wurde.

16.01.2021

Ort, Datum

Rongrui Na

Unterschrift Doktorand in bzw. Doktorand